Since January 2020 Elsevier has created a COVID-19 resource centre with free information in English and Mandarin on the novel coronavirus COVID-19. The COVID-19 resource centre is hosted on Elsevier Connect, the company's public news and information website.

Talanta 253 (2023) 124051

Contents lists available at ScienceDirect

Talanta

journal homepage: www.elsevier.com/locate/talanta

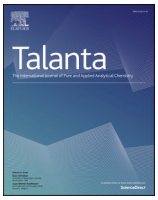

Sandwich mode lateral flow assay for point-of-care detecting SARS-CoV-2

Fubin Pei [a,b], Shasha Feng [a,b], Wei Hu [b], Bing Liu [b], Xihui Mu [b], Qingli Hao [a], Yang Cao [a], Wu Lei [a,*], Zhaoyang Tong [b,**]

[a] School of Chemistry and Chemical Engineering, Nanjing University of Science and Technology, Nanjing, 210094, Jiangsu, China
[b] State Key Laboratory of NBC Protection for Civilian, Beijing, 102205, China

ARTICLE INFO

Keywords:
Lateral flow assay
SARS-CoV-2
Immunoassay
Point-of-care

ABSTRACT

The global corona virus disease 2019 (COVID-19) has been announced a pandemic outbreak, and has threatened human life and health seriously. Severe acute respiratory syndrome coronavirus 2 (SARS-CoV-2), as its causative pathogen, is widely detected in the screening of COVID-19 patients, infected people and contaminated substances. Lateral flow assay (LFA) is a popular point-of-care detection method, possesses advantages of quick response, simple operation mode, portable device, and low cost. Based on the above advantages, LFA has been widely developed for detecting SARS-CoV-2. In this review, we summarized the articles about the sandwich mode LFA detecting SARS-CoV-2, classified according to the target detection objects indicating genes, nucleocapsid protein, spike protein, and specific antibodies of SARS-CoV-2. In each part, LFA is further classified and summarized according to different signal detection types. Additionally, the properties of the targets were introduced to clarify their detection significance. The review is expected to provide a helpful guide for LFA sensitization and marker selection of SARS-CoV-2.

1. Introduction

The corona Virus Disease 2019 (COVID-19) outbreak began in 2019, and its virus was denoted as severe acute respiratory syndrome coronavirus 2 (SARS-CoV-2) [1]. Due to high infectivity and wide transmission routes, it was declared a pandemic in March 2020. About 553 million confirmed cases and over 6.3 million deaths were reported worldwide, according to the World Health Organization (WHO) report on July 13, 2022. Each country has invested a great deal of manpower and resources in the development of COVID-19 vaccines, prevention and treatment strategies, making a great contribution to preventing the spread of the epidemic and treating patients. SARS-CoV-2 virus is composed of single-stranded ribonucleic acids (RNA) and four structural proteins, including the spike (S), membrane (M), envelope (E) and nucleocapsid (N) proteins [2,3]. A schematic is shown in Fig. 1. Among them, the genes from RNA, S protein, N protein, and specific antibodies (including neutralizing antibodies, IgG, IgM, and IgA *etc.*) are selected as markers for detecting SARS-CoV-2. However, the E and M proteins are difficult to extract, detect, and identify due to being relatively short and tightly membrane-bound, which results few methods detecting them [4].

As we all know, controlling the source of infection and protecting the susceptible population are the two important measures to prevent infectious diseases. The premise of both measures is to identify whether a person has been infected with the virus. Nevertheless, the large number of screening groups, inconspicuous symptoms in the initial infection, and asymptomatic patients make screening more difficult. Currently, three different types of diagnostic strategies are being used to diagnose COVID-19, including chest computed tomography (CT) scan, reverse transcription-polymerase chain reaction (RT-PCR) assay, and lateral flow assay (LFA) [5]. CT requires large and expensive equipment, and professional technicians, which is not convenient for primary screening of large numbers. RT-PCR requires specially trained technicians to operate machines for several hours [6].

LFA, also called simply strip test or immunochromatographic assay, possesses the advantages of simple usage patterns, short time-consumption, good long-term stability and low cost, thus it is a widely used point-of-care testing detection method [7,8]. Typically, the LFA consists of a sample pad (onto which the sample to be tested is loaded), conjugate pad (containing the labeled bio-recognition molecule to the target), nitrocellulose (NC) membrane (immobilizing the capture and control molecule), and absorbent pad (providing the capillary force) [9].

* Corresponding author.
** Corresponding author.
E-mail addresses: leiwuhao@njust.edu.cn (W. Lei), billzytong@126.com (Z. Tong).

https://doi.org/10.1016/j.talanta.2022.124051
Received 4 August 2022; Received in revised form 21 October 2022; Accepted 24 October 2022
Available online 27 October 2022

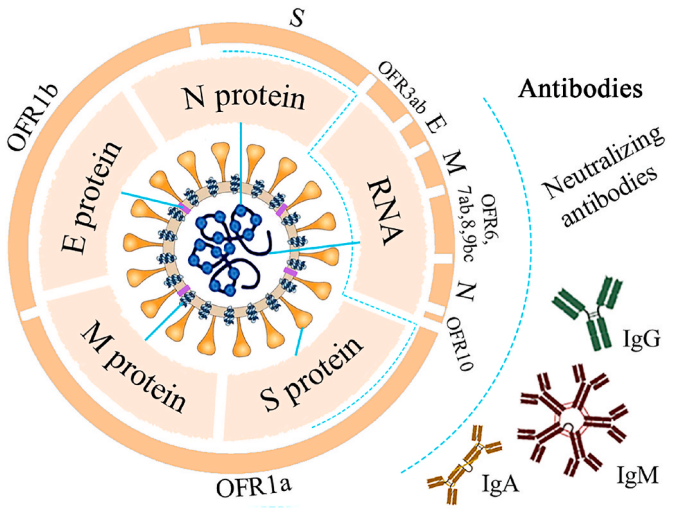

Fig. 1. The structural schematic of SARS-CoV-2 virus, RNA, and specific antibodies.

During detection, the sample solution is moved through the membrane towards the absorbent pad by capillary force; the labeled bio-recognition molecules are captured on the test (T) line after binding to the target analytes, which can achieve significant color changes [10]. Responses can also be converted into fluorescence, Raman, chemiluminescence (CL) and magnetic signals to achieve qualitative and quantitative assays [7].

Based on the above advantages, a large number of LFA for SARS-CoV-2 detection have been reported. Pérez-López and Mir [11] reviewed the research on commercialized diagnostic technologies to combat SARS-CoV-2 indicating genosensors and immunosensors, and introduced the advantages of various detection methods. Ernst et al. [12] summarized against SARS-CoV-2 serology assay platforms, helping people to know more about antibodies detection. The reviews [13–16] were involved a variety of detection methods, such as computed tomography scan, nucleic acid amplification test, LFA, ELISA, played a guiding role in the subsequent research on SARS-CoV-2 detection. However, these reviews only take LFA as a part, which cannot fully interpret the advantages and research progress of LFA for SARS-CoV-2. Zhou et al. [17] reviewed LFA for SARS-CoV-2 nucleic acids, antigen, antibody, and elaborated its advantages and disadvantages, which has greatly facilitated the review on LFA for SARS-CoV-2. With the development of materials science and more attention to LFA, a large number of new LFA for SARS-CoV-2 researches have emerged. It is very necessary to review the research on LFA for SARS-CoV-2 detection.

Herein, we focus on reviewing the recent progress in the application of sandwich mode LFA for detecting genes, N protein, S protein, and antibodies of SARS-CoV-2. This review introduces the properties of the targets to clarify their detection significance, and classifies the research on LFA according to the targets to summarize the current situation. Furthermore, strategies of sensitization are reviewed in order to provide some reference value for sensitization of LFA for SARS-CoV-2. The typical studies with characteristics in each classification are also introduced. Among of them, LFAs for SARS-CoV-2 genes were summarized according to gene processing techniques, which complemented the contents of Castrejón-Jiménez et al. [18] review. At the end of the review, the challenges and future research directions of LFA for SARS-CoV-2 were predicted.

2. Signal output and amplification strategies of LFA

Gold nanoparticles (Au NPs) possess advantages of simple preparation method, uniform particle size, and good stability, widely applied in biosensor, especially Au NPs colloidal solutions [19]. Au NPs colloidal solutions emerge red color owing to localized surface plasmon resonance [20]. Additionally, Au NPs can bind antibodies by gold ammonia bond or electrostatic adsorption [21,22]. Based on the above advantages, they have been regarded as the ideal material for colorimetric LFA via naked-eye detection. Due to simple production, low cost, good semi-quantitative performance, and simple naked eye detection mode, colloidal gold LFA has been achieved mass commercial production. In order to realize quantitative detection and signal sensitization, fluorescence, surface enhanced Raman scattering (SERS), CL, and magnetic LFA have been invented.

2.1. Signal output types

2.1.1. Colorimetric LFA

Colorimetric LFA usually uses measurement of color changes to determine the amount of analytes in samples [23]. Generally, most of the nanomaterials with dark color, uniform size, and the ability to bind antibodies antibody, can be used for colorimetric LFA. In view of colloidal Au NPs excellent characteristics, they are the most widely used material for constructing colorimetric LFA. Colorimetric LFA possesses notable advantages including simple instruments, high portability, simple operation, and fast detection by naked eyes, especially in rapid and on-site detection [24]. Nonetheless, the mode of naked eye detection limits it to semi-quantitative or qualitative detection. Color recognition software has employed to quantify the content of analysts via the color of the immune complex on T lines, such as grayscale, RGB, and HSV [25].

2.1.2. Fluorescent LFA

Fluorescent technique with simplification, high sensitivity, and strong operability is among the most popular optical sensing strategy [26]. Detection of fluorescence emission pattern is more sensitive than light absorption [27]. Additionally, a uniform background is achieved owing to the efficient blocking of the excitation light [28]. Thus, fluorescence system has higher sensitivity than observation system, and promises lower limits of detection. Smartphone-based fluorescence reader, integrating the smartphone with electrical components or external optical, reduces complexity and realizes miniaturization [29].

2.1.3. SERS LFA

SERS is a promising technique, displays the advantages of rapidity, convenience, extraordinary sensitivity, and nondestructive [30,31]. Moreover, the fluorescence quenching and photobleaching are avoided via the long-wavelength excitation effectively [32]. Typically, SERS nanotags consist of the enhanced substrate (Au/Ag nanoparticles), Raman dye molecules, and specific antibodies [33]. Raman dye molecules including 5,5′-dithiobis(2-nitrobenzoicacid) (DTNB), 4,4′-dipyridyl (44DP), phthalazine (PHTH), 1,2-bis(4-pyridyl)-ethylene (12BE), and, 2,2′-dipyridyl (22DP) provide strong and specific SERS signal [34,35]. SERS signal originating from the rotation and vibration of dye molecule is more stable and single nanotag may be detected [36]. SERS based LFA possesses the advantage of simplicity, portability, speediness, and high sensitivity [37].

2.1.4. Magnetic LFA

Giant magnetoimpedance (GMI) effect caused by the skin effect is a large change in the impedance of the alternating current in a soft magnetic material during an external magnetic field applied [38]. GMI sensors possess advantages of low cost, higher sensitivity, low power consumption, repeatability, resistance to mechanical vibration, and simple convenience [39]. Compared with colorimetric method, the magnetic signal has good anti-interference from sample matrix [40]. Therefore, GMI based LFA shows great potential.

2.2. Signal amplification strategies

2.2.1. Material-based signal amplification

There is no doubt that the rapid development of nanotechnology and materials science has laid a strong foundation for the development and innovation of LFA. Improving material properties to amplifying LFA signal is an effective signal amplification strategy, which attracted much attention from researchers [41]. The strategies for improving the performances of material used in LFA can be broadly divided into three types. The characteristics such as the proportion of crystal plane, Fermi level, color, *etc*. can be adjusted by the strategy of changing the morphology, size and crystal form of the material to obtain the material with the best performance. Two or more kinds of materials are combined to produce high performance composite materials with synergistic effects of each component. Finally, increasing the proportion of active ingredients in loaded materials makes them more efficient.

2.2.2. Chemical enhancement LFA

Nanozyme is nanomaterial with enzyme-like activity, expresses many advantages of strong catalytic activities, low cost, sustainability, stability, and robustness [42–44]. Peroxidase-like catalyzes decomposition of hydrogen peroxide (H_2O_2), which can oxidate 3,3′,5,5′-tetramethylbenzidine (TMB) to color, and catalyze luminol oxidation to produce intensified CL [45,46]. Those chromogenic with high efficiency oxidation produce chromogenic products even on trace amounts of targets [47]. Introducing the nanoenzyme chromogenic reaction into LFA can expand detection range and reduce the detection limit.

2.2.3. Nucleic acid amplification improving LFA

In addition to the above two methods, increasing the content of the substance to be measured in the detection sample is also a strategy to improve the detection signal intensity when other conditions are unchanged [48]. It is difficult to increase the concentration of protein target such as antigen and antibody in the detection sample. Nucleic acid can be amplified by RT-PCR, recombinase polymerase amplification (RPA), and reverse transcription loop-mediated isothermal amplification (RT-LAMP) *etc.* to increase the target detection gene fragment in the sample [49–51]. The amplified sample has a higher content of target, which can play a role in amplifying the sensor signal.

3. LFA for SARS-CoV-2

This section is divided into four subsections: LFA for the detection of genes, N protein and S protein of SARS-CoV-2 virus, and specific antibodies produced by host cells with SARS-CoV-2 infection. The properties of the four kinds of targets are introduced. Moreover, recently developed LFAs are classified and summarized, according to detection methods. We hope that this section can not only facilitate the understanding of the research development, but also provide guidance for the selection of target for SARS-CoV-2 and provide ideas for the future study of LFA sensitization.

3.1. LFA for RNA of SARS-CoV-2 detection

The genome of SARS-CoV-2 is a single-stranded positive RNA, its length is about 30 kilobases, including a 5′ cap structure and a 3′ poly(A) tail [52,53]. The open reading frames (ORFs) called ORF1a and ORF1b occupy two-thirds of the length the RNA genome of SARS-CoV-2 at the 5′ end, and encode polyproteins (PP1ab and PP1a) [54,55]. Polyproteins are precursors for 16 non-structural proteins and perform a fundamental role in viral transcription, replication, and immune response modulation [56]. The remaining genome encodes four important structural proteins (S, E, M, and N genes) and nine accessory proteins (ORF3a-10) [57]. These structural proteins as an important part of the SARS-CoV-2 virus and play a significance role in viral entry into the host cell [58]. Accessory proteins are involved in virulence and pathogenesis [58]. Detection of RNA has the advantage of accurate identification. However, the low content requires amplification prior to be detection, necessitating RT-PCR, RPA, and RT-LAMP, *etc*. Moreover, the clustered regularly interspaced short palindromic repeats associated protein (CRISP/Cas), is an attractive gene detection tool, and when combined with nucleic acid amplification methods has been employed in genetic diagnosis. Here, we review the sandwich type LFA detecting genes of SARS-CoV-2 by different strategies of amplification.

3.1.1. FLA combined with RT-PCR

RT-PCR is one of the most common methods for gene amplification [59]. In brief, the RNA is reverse transcribed into cDNA by reverse transcriptase and the cDNA template amplified. It can greatly improve the sensitivity of RNA detection. Dighe et al. [60] reported a gold nanoparticle FLA combined with RT-PCR for detection of the N genes of SARS-CoV-2. They found that cysteamine capped Au NPs as signal source increased the visibility of the T line. The assay can detect 0.02 copies/μL of SARS-CoV-2 genomic RNA, and its specificity and accuracy were 99.99%. Kim's group [61] first reported a fluorescence lateral flow strip membrane assay to detect SARS-CoV-2 by targeting more than one gene. This method can simultaneously detect RdRp, ORF3a, and N genes using the Cy5-labeled PCR product from the single-tube RT-PCR in 30 min. The detection limit was 10 copies/test for each gene. Moreover, Wang et al. [62] developed red or green color magnetic-quantum dot nanobeads (QBs)-based fluorescent LFA for discriminating D614G and N501Y gene segments from wild-type (WT) or mutated (M) SARS-CoV-2. The tetra-primer amplification refractory mutation system (ARMS) combined with PCR was used to amplify the gene segments. The T1 and T2 line can capture D614G and N501Y. The D614G and N501Y of WT bind green QBs, and M bind red QBs. The schematic and detection diagram is shown in Fig. 2. The assay can be completed in less than 2 h, and the LOD was 33.53 copies/μL for M D614G. The LFA also can detect the N and ORF1ab genes of SARS-CoV-2, simultaneously. The LODs for the N and ORF1ab genes (on red and green channel) were 1.90 copies/μL and 6.07 copies/μL, respectively. The detection mode of LFA with double T lines can achieve dual signal or dual target detection at the same time, can greatly save the cost and test time, compared with the single T-line.

3.1.2. FLA combined with RPA

RPA is promising isothermal molecular amplification tool with operation simplicity and short detection time [63]. Recombinase is used to assist primer annealing for strand elongation during amplification resulting in a lower temperature being needed for than RT-PCR [64]. Farrera-Soler et al. [65] combined RPA with a nucleic acid-templated nucleophilic aromatic substitution to achieve a dual readout with fluorescence microtiter plate or colloidal gold LFA. The LFA can detect the ORF1b (nucleotides 15,418–15,554) of the SARS-CoV-2 genome 250 pM being visible by the naked eye. In contrast to RPA, quantitative RPA (qRPA) is a competitive amplification with a known concentration of reference molecules. The qRPA combined with a triple-line lateral flow assay for N genes of SARS-CoV-2 based on Au NP-labeled anti-FAM antibodies was reported by Springer's group [66]. The input concentration was inferred by the ratio of target and reference amplicons. The biotinylated probe hybridized with the target sequence, and the digoxigenin labeled probe hybridized with the reference sequence. Results were captured by a streptavidin band (T line) and an anti-digoxigenin band (reference line) on LFA, respectively. The analysis process is represented graphically in Fig. 3. This construction mode enriches LFA for nucleic acid and is conducive to the diversity of its development. And its sensitivity and specificity was 95% and 97% for 58 samples. Moreover, Li's team [67] reported duplex reverse transcription-RPA (RT-PRA) integrated colorimetric LFA to detect ORF1ab and N genes. T1 and T2 lines were utilized to capture amplification product from each. The assay with the accuracy of 100% clearly distinguished 10 copies/test of the ORF1ab and N gene templates from a blank control.

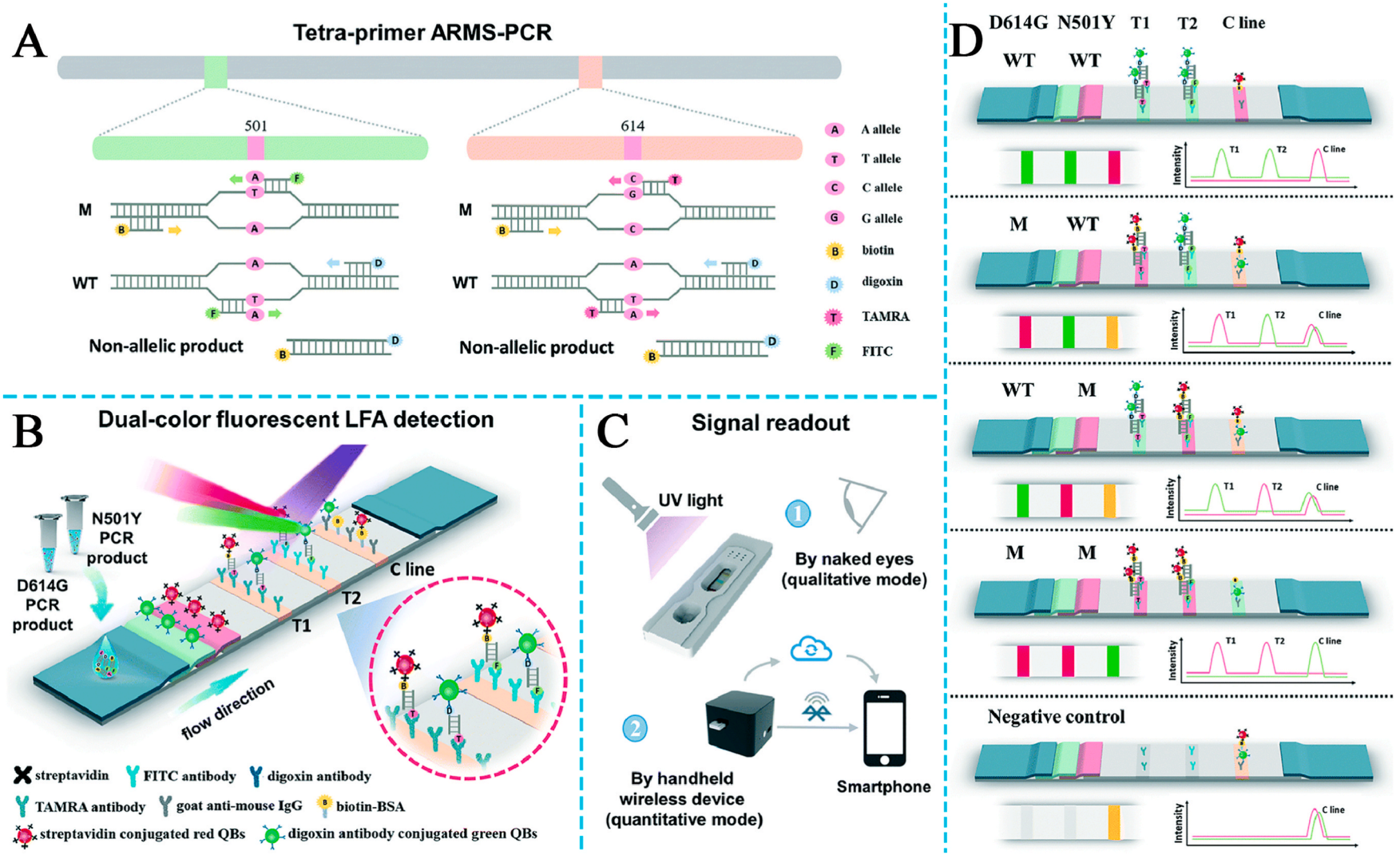

Fig. 2. Schematic of dual-color QBs-based fluorescent LFA: Tetra-primer ARMS-PCR (A); Dual-color QBs-based fluorescent LFA (B); Signal readout (C); Interpretation of the representative test results of lateral flow strips (D) [62]. (For interpretation of the references to color in this figure legend, the reader is referred to the Web version of this article.)

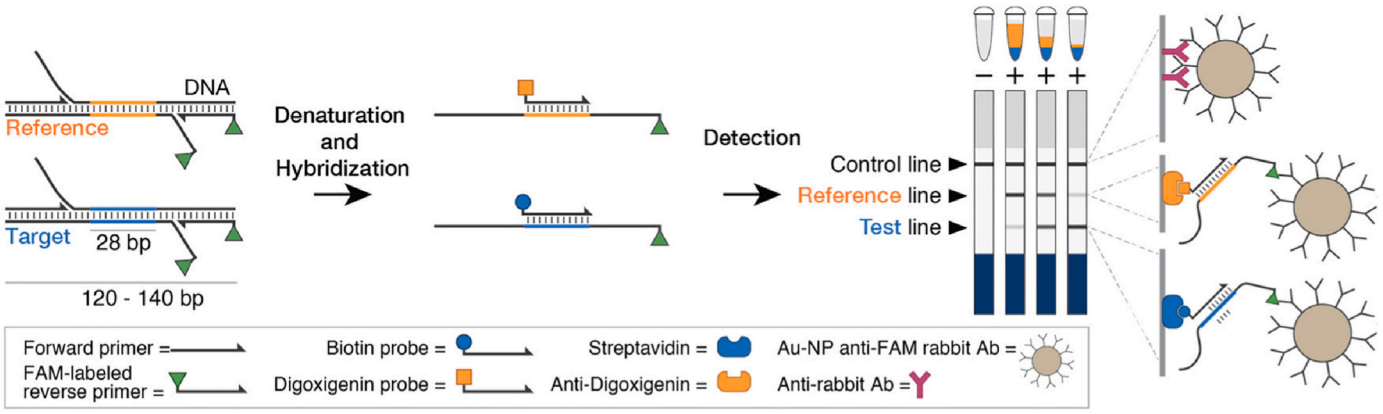

Fig. 3. Target and reference amplicons detected via hybridization probes and visualized on LFA [66].

3.1.3. FLA combined with RT-LAMP

RT-LAMP is based on isothermal nucleic acid amplification, and realizes a one-step gene amplification [68]. It has short run-times, low cost, good robustness, strong resistance, and simple operator, operation and has attracted particular attention for bioassays [69,70]. Zhang et al. [71] used RT-LAMP to amplify the ORF1ab and N genes and employed Au NPs LFA to visualize amplification results with the accuracy of 97.2%. The method produced clear signals with a concentration of ORF1ab or N genes of not lower than 2 copies/μL. Furthermore, Li's team [72] developed a four-channel microfluidic device to combine RT-LAMP with commercial Au NPs LFA for M or N genes of SARS-CoV-2. The microfluidic channel had two zones (indicating amplification and incubation) and three pressure-vent pores. The whole assay comprised injecting the sample lysis into A pores, heating injecting the hCG-Ps via B pores, incubating, pushing to puncture, and detection by naked eye. The schematic of the assay is shown in Fig. 4. The device was about the size of a hand, and showed sensitivity as low as 0.5 copies/μL. The portable device achieved gene amplification and detection, greatly reducing the use of instrumentation and promoting the development of portable and commercial of LFA based on gene amplification. A multiplex RT-LAMP coupled with dye streptavidin coated polymer nanoparticles LFA for detecting ORF1ab and N genes simultaneously was devised by Wang's group [73]. The assay can be completed within 1 h, and had a limit of detection of 12 copies/reaction. Banerjee et al. [74] developed a platform technology combined RT-LAMP, hybridization technique and Au NPs LFA for RdRp, or N, or E genes. The limit of detection was suggested to be 100 copies/μL.

3.1.4. FLA combined with other amplification strategy

Zhuang et al. [75] designed a pair of adjacent amplification primers for target gene, and the enhanced reverse transcription primers also were templates during isothermal amplification, named as enhanced strand exchange amplification (ESEA). They introduced a fluorescence LFA combined with ESEA to detect the RdRp or N genes, respectively. The assay fluorescent microspheres were used as signal source, and could be completed within 1 h. The sensitivity of the method was 90 copies/μL and 70 copies/μL for the RdRP and N genes respectively. Catalytic hairpin assembly (CHA) is a nonenzymatic nucleic acid isothermal amplification versatile tool. Due to low background, high efficiency, and easy operation, it is widely employed for developing biosensors [76,77]. Fan's team [78] developed a method based on a CHA reaction coupled with LFA for ORF1ab or N genes, the fluorescent signal from Alexa Fluor 647. The method showed a minimum detectable concentration of 10 aM for ORF1ab or N genes.

3.1.5. FLA combined with CRISPR-Cas

CRISP/Cas is a gene editor triggered by specific target recognition. Due to high base resolution, economy, and isothermal signal amplification, it is considered the tool of choice for genome editing [79]. Developing a system of CRISPR/Cas combined with LFA may realize field detection with low cost and high sensitivity [80]. The following typical reports are selected for review and the remaining studies can be found in Table 1.

Yi's group [81] reported a quantum dot microsphere fluorescent LFA combined with reverse transcription, isothermal amplification, and CRISPR/Cas13a for the S gene of SARS-CoV-2. It showed the detection limit of 1 copy/mL. Multi-genomic tests have been extensively studied to reduce the false-negative of single genomic tests [61]. Zhu et al. [82] developed a LFA based on reverse transcription multiple cross displacement amplification combined with CRISPR/Cas12a-based detection for the ORF1ab or N genes of SARS-CoV-2 with the accuracy of 100%. Au NPs were used to develop color for LFA, and the sensitivity was as low as 7 copies/test. Additionally, the whole test took less than 1 h. Hou et al. [83] also reported LFA based on CRISPR/Cas13a for ORF1ab or S genes. Interestingly, they developed a fluorescent analyzer with a 3D-printed microfluidic chip to address aerosol contamination issues. A schematic illustration for detecting ORF1ab or S genes of SARS-CoV-2 is presented in Fig. 5. The analyzer possessed advantages of portability, automation, high-throughput, and high accuracy. The LOD for ORF1ab and S genes was 20 fM and 2 fM, respectively. Moreover, a fluorescent analyzer with a 3D-printed microfluidic chip was developed with LOD for ORF1ab and S genes of 4.16 fM and 0.68 fM, respectively. The two detection methods complement each other, and the accuracy of sensor can be improved by comparing the results of the two detection methods in the overlapping detection range.

Zhou et al. [84] published a method for simultaneous detection of ORF1ab and E genes via CRISPR/Cas9-mediated LFA combined with multiplex reverse transcription-recombinase polymerase amplification (RT-RPA). Au NP-DNA probes, streptavidin, anti-digoxin antibodies, and probes conjugated with streptavidin were pre-embedded on conjugate pad, T1, T2, and C line, respectively. The whole detection including sample collection, RNA extraction, multiplex RT-RPA reaction, CRISPR-Cas9 reaction, and the lateral flow assay took less than 1 h. A schematic of amplification and detection results is shown in Fig. 6. The assay had a sensitivity of 100 copies/reaction (25 μL), 100% negative and 97.14% positive predictive agreement for 64 clinical samples.

In order to facilitate quick view, the literatures reviewed are summarized in Table 1. We find that CRISPR is an emerging gene processing method, which has been widely used in LFA for SARS-CoV-2 gene detection after combining with gene amplification technology. Among the LFA for gene detection, colorimetric LFA occupies an important place, and the number of studies far exceeds that of fluorescent LFA. Additionally, the maximum detection range of colorimetric LFA can span 7 orders of magnitude. There are still many studies on LFA for gene detection based on Au NPs, and its LOD can reach 2 copies/reaction. The ORF occupying the longest nucleic acid chain and the N gene encoding

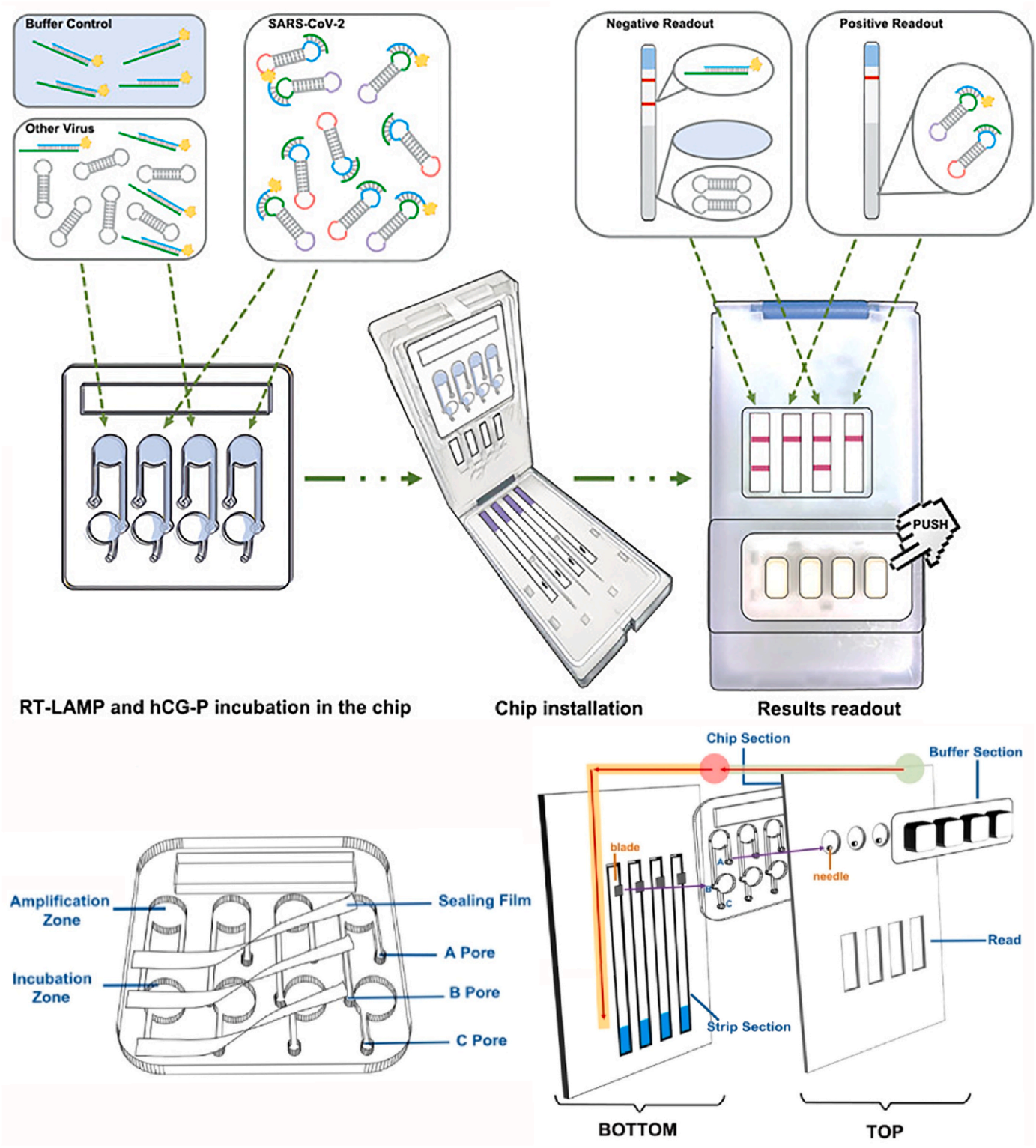

Fig. 4. The schematic of the assay, structure of the microfluidic chip, and different units of the portable device [72].

the nuclear protein are the main detection objects. The broadest detection range of the LFA based on quantum dot microspheres can span 6 orders of magnitude. Nucleic acid is the most representative substance of virus, and nucleic acid amplification technology can continuously improve the concentration of target detection, which gives the LFA of nucleic acid detection a high credibility. Nucleic acid amplification requires specialized equipment and professional operation to complete the screening of large numbers of people using long time, which limits the application of its outdoor, rapid, and self-detection models.

3.2. *LFA for SARS-CoV-2 N protein detection*

N protein is a structural protein of molecular weight about 40 kDa [88,89]. N protein binds to the viral genome, producing helical ribonucleoprotein complexes to promote the correct folding of the hammerhead ribozyme avoiding unproductive RNA conformations

Table 1
LFA for RNA of SARS-CoV-2.

Manipulate genes technology	Detection method	Target genes	Signal material	Detection range	LOD	Specificity (%)	Reference
RT-PCR	Colorimetry	N	Cysteamine capped Au NPs	0.001–67,250 copies/μL	0.02 copies/μL	99.99	[60]
	Fluorescence	RdRp, ORF3a, and N	Cy5	10–1000 copies/reaction	10 copies/reaction	–	[61]
	Fluorescence	N and ORF1ab	Red or green color magnetic-QBs	50–500,000 copies/reaction	9.50 and 30.35 copies/reaction	–	[62] [a]
RPA	Colorimetry	ORF1b	Au NPs	–	20 copies/reaction	–	[65] [a]
	Colorimetry	N	Au NPs	–	–	97	[66]
	Colorimetry	ORF1ab and N	Red carboxyl modified latex microspheres	10–100,000,000 copies/reaction	10 copies/reaction	–	[67]
RT-LAMP	Colorimetry	ORF1ab and N	Au NPs	–	50 copies/reaction	100	[71]
	Colorimetry	M or N	Au NPs	–	2 copies/reaction		[72]
	Colorimetry	ORF1ab and N	Dye streptavidin coated polymer nanoparticles	0.012–12,000 copies/reaction	12 copies/reaction	100	[73]
	Colorimetry	RdRp, N, or E	Au NPs	–	1000 copies/reaction	100	[74] [a]
ESEA	Fluorescence	RdRp or N	Fluorescent microspheres	270–270,000 or 210–210,000 copies/reaction	270 or 210 copies/reaction	–	[75] [a]
CHA	Fluorescence	ORF1ab or N	Alexa Fluor 647	2–2,000,000 copies/μL	2 copies/μL	–	[78]
CRISPR/Cas9	Colorimetry	ORF1ab and E	Au NPs	–	100 copies/reaction	–	[84]
CRISPR/dCas9	Colorimetry	ORF1b or N	Au NPs	100–10,000 copies/reaction	100 copies/reaction	–	[85]
CRISPR/Cas12a	Colorimetry	ORF1ab or N	Au NPs	7–70,000 copies/reaction	7 copies/reaction	–	[82]
	Fluorescence	N501Y, D614G, or 69/70 deletion	Tecan's Spark 20 M	1200–120,000, 1200–12,000, or 120–12,000 copies/reaction	120, 120, or 12 copies/reaction	–	[86] [a]
CRISPR/Cas12b	Colorimetry	ORF1ab or N	Au NPs	10–1,000,000 copies/reaction	10 copies/reaction	100	[87]
CRISPR/Cas13a	Fluorescence	S	Quantum dot microspheres	–	–	100	[81]
	Colorimetry	ORF 1 ab or S	Au NPs	0.02–200 pM or 0.002–20 pM	20 or 2 fM	–	[83]

[a] The concentration was converted via the volume of gene template added before amplification.

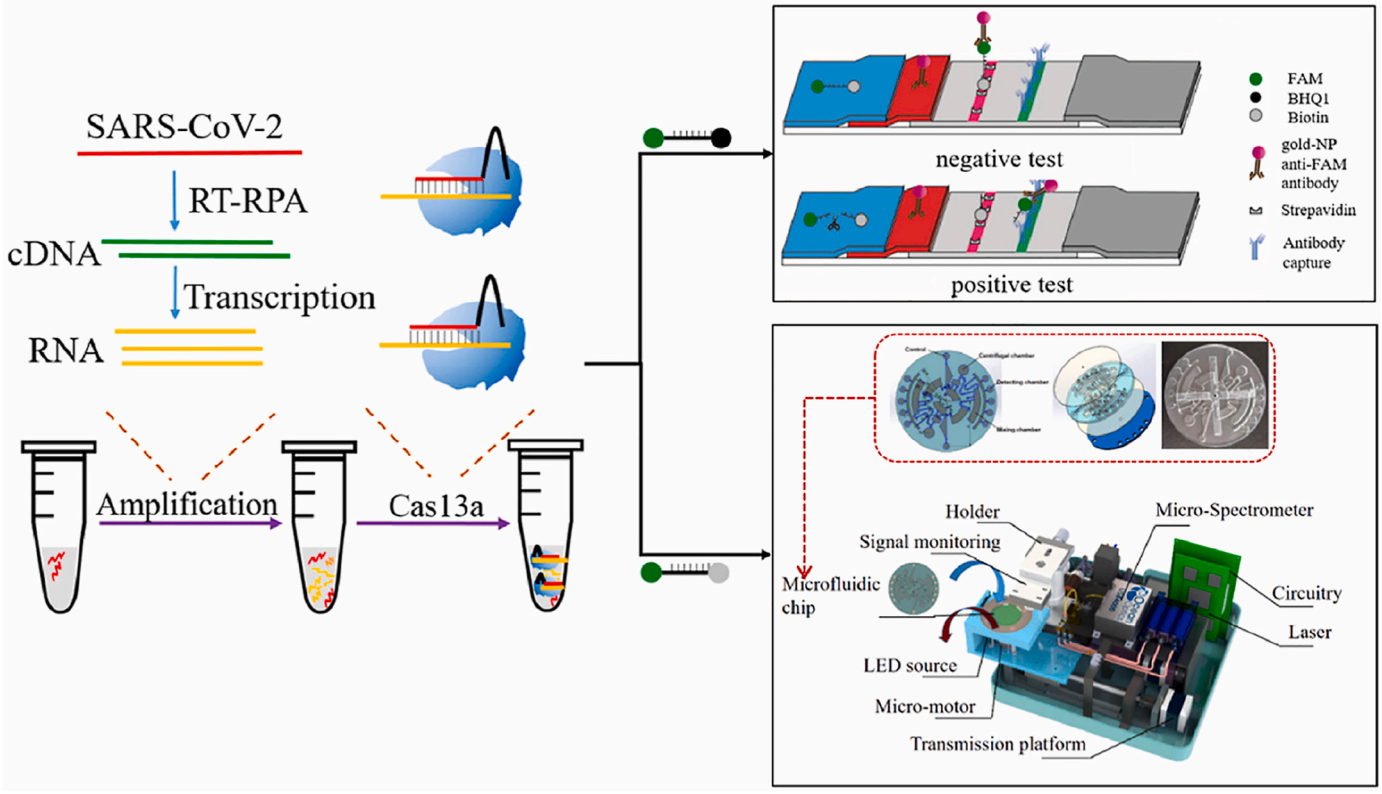

Fig. 5. Schematic illustration for detecting SARS-CoV-2 strategy [83].

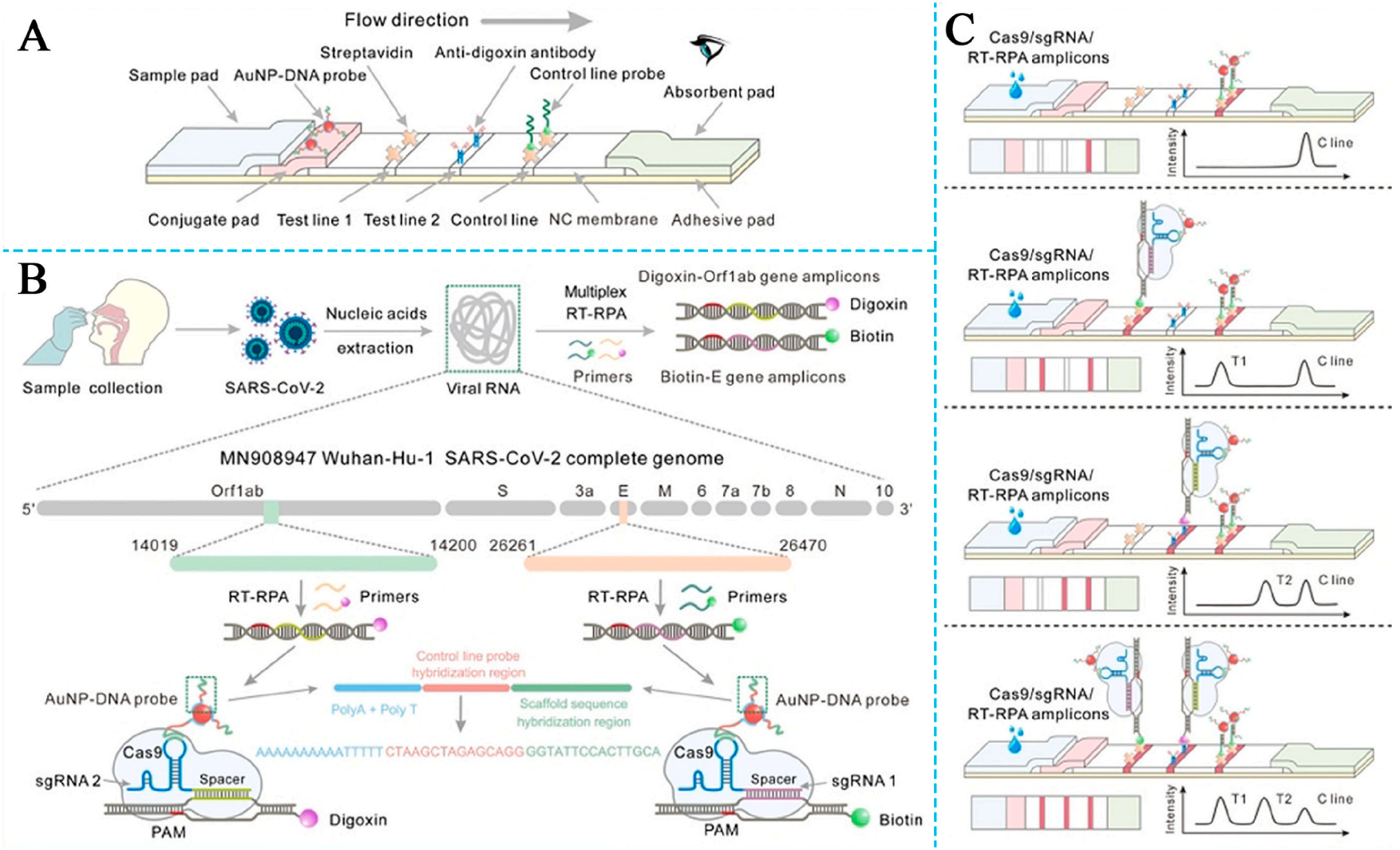

Fig. 6. Schematic of the CRISPR/Cas9-mediated triple-line LFA [84].

[90]. As the only viral structural protein in the replicase-transcriptase complex, it is also plays a pivotal role in RNA synthesis with components of the replicase [91–93]. Additionally, it can regulate cellular processes, for instance actin reorganization, cell cycle progression, and the immune response [94]. The diversity of N protein amino acid sequence fluctuates far less over time and geography [95]. Although it exists within the viral particle, the N protein is highly immunogenic and will be abundantly expressed in patients with SARS-CoV-2 infection [96, 97]. Thus, N protein is considered a suitable target for antigen testing [98], and can be used for COVID-19 diagnosis, according to the WHO [99].

At present, there has been little research into LFAs for detecting the N protein of SARS-CoV-2, and the main methods include colorimetric, fluorescent, simulated enzyme chromogenic and photothermal enhancement. Hyun-Kyung Oh et al. [100] developed a colorimetric lateral flow platform based on plasmon color-preserved Au NPs clusters to detect SARS-CoV-2 nucleocapsid protein. The Au NP clusters were formed by mixing streptavidin-coated Au NP (d = 40 nm) core with satellite Au NPs (d = 40 nm) covered by biotinylated antibodies. A schematic of signal materials and detection results are shown in Fig. 7. The distance between the Au NPs composed of nanoclusters is about 15 nm resulting in the avoidance of plasmon coupling and increasing the overall light absorption. Its detection range was from 30 pg/mL to 1000 ng/mL, and its LOD was 38 pg/mL, 23.8 times that of single 15 nm Au NPs. This is a great innovation of the traditional colloidal gold colorimetric LFA, which greatly improves the sensitivity of detection and reduces the LOD. It also provides a new idea for the sensitization study of colorimetric LFA. Zhao et al. [101] also fabricated a colorimetric LFA to detect the N protein of SARS-CoV-2 based on red latex microspheres as the signal source, with LOD of 25 ng/mL and the specificity of 97.93.

Ding's group [102] used the red emission of carbon dots enriched in silica spheres to develop a fluorescent LFA for SARS-CoV-2 N protein. Under the fluorescence microscope, the limit of detection was as low as 10 pg/mL. Wang et al. [103] reported the development of a dual-target fluorescent LFA comprising two test lines, to detect the N and S proteins simultaneously based on magnetic quantum dot with a triple-CdSe/ZnS-MPA QDs shell (MagTQD). The schematic diagram of the MagTQD preparation and detection process is shown in Fig. 8. Due to the high fluorescence performance of MagTQD, its limit of detection for N and S protein was 0.5 pg/mL. Compared with other studies, this study has a lower LOD and a wider detection range, which has greatly encouraged LFA researchers to invest in the research of quantum dots enhanced fluorescent LFA. We believe that with the further research, more quantum dots will be used to sensitize fluorescent LFA and achieve good performance. Additionally, Xie et al. [104] fabricated a magnetic/fluorescent dual-modal LFA for SARS-CoV-2 N protein based on a composite of Fe_3O_4 core with CdSe/ZnS QDs shells. The detection ranges were 0.5–1000 ng/mL or 0.05–500 ng/mL, LODs were 0.235 or 0.012 ng/mL for magnetic signal or fluorescent signal, respectively. This study proves that the fluorescence LFA based on quantum dots has high sensitivity, and the proposed strategy of double detection signals helps to improve the accuracy of detection. Aggregation-Induced Emission (AIE) results in the fluorescence of molecules in a solid or aggregated state, overcoming quenching due to aggregation, and has attracted wide attention [105]. Zhang et al. [106] developed an AIE luminogens based lateral flow test strip for detection of N or RBD protein from SARS-CoV-2, based on the AIE fluorescence molecule synthesized by Knoevenagel condensation. The LODs were 7.2 and 6.9 ng/mL for N and receptor-binding domain (RBD) protein and anti-interference capacity was higher than that of the test strip based on Au NPs or fluorescein isothiocyanate.

A half-strip LFA does not have sample or conjugate pads, by contrast with LFA. It is a helpful first step in LFA development. Benjamin D. Grant et al. [107] presented a half-strip LFA to detect SARS-CoV-2 N protein based on 400 nm carboxylic red and blue latex beads.The LOD was 0.65 ng/mL for the Genemedi N protein measured by a commercial optical LFA reader. Furthermore, Bradbury et al. [108] fabricated a nanozyme signal enhancement LFA for the SARS-CoV-2 N protein based on platinum-coated gold nanozymes (Au@Pt NZs). A novel device composed of LFA test strip, dehydrated signal enhancement reagents, and a casing with stored liquid, was developed to standardize of test results. A schematic showing the detection process is vividly illustrated in Fig. 9. Due to TMB as substrate enhancing the LFA signal, the LOD has been increased by ten-fold to 0.1 ng/mL. In addition, a casing made by 3D printing was used to enhance reagent storage and delivery for LFA. The device simplifies the sensitization process, which is conducive to the standardization of detection of enzyme sensitization LFA. Photothermal detection (PTD) of nanoparticles is also used in LFA. Chang's research team [109] developed a portable LFA reader based on PTD. A low-power green laser and a single-element infrared sensor were employed as the heating source and detector to increase the portability of the LFA reader. The reader can detect of SARS-CoV-2 N protein captured by immune colored latex beads on LFIA strips with a LOD of 0.13 ng/mL. Although the LOD is not as low as with fluorescence, these studies provide a new idea for enhancing sensitivity of traditional colloidal gold LFA.

3.3. LFA for SARS-CoV-2 S protein detection

The S protein of SARS-CoV-2 virus is a large heavily-glycosylated transmembrane protein consisting of 1273 amino acids [115]. It exists as a trimer on the surface of virus, and plays an important role in preventing antibody recognition and facilitating immune evasion [116].

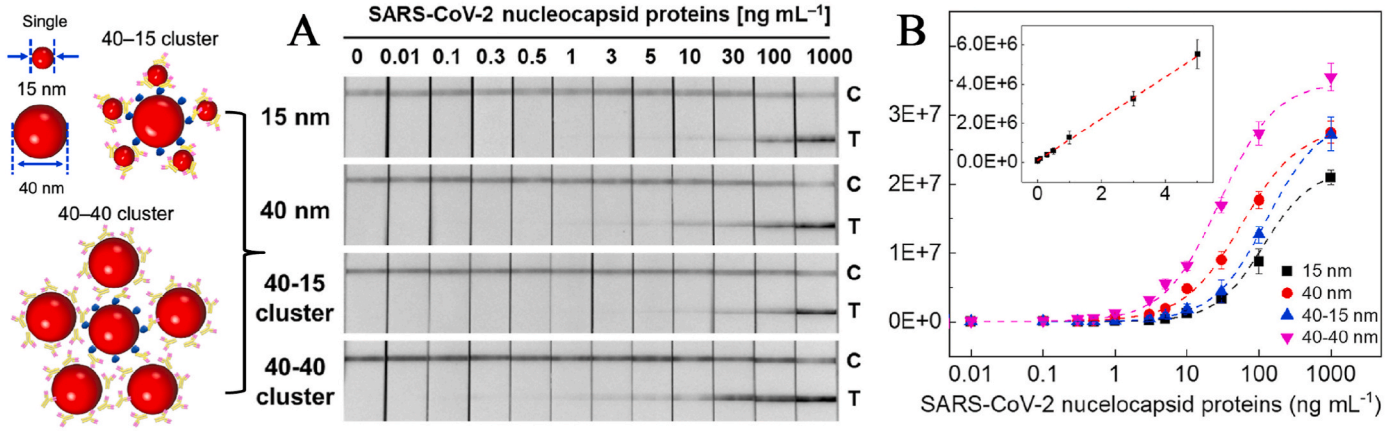

Fig. 7. The colorimetric LFA for SARS-CoV-2 N protein based on Au NPs (15 nm and 40 nm) and Au NP clusters (40–15 and 40-40 clusters), respectively (A); Their T line fitting curve (B) [100].

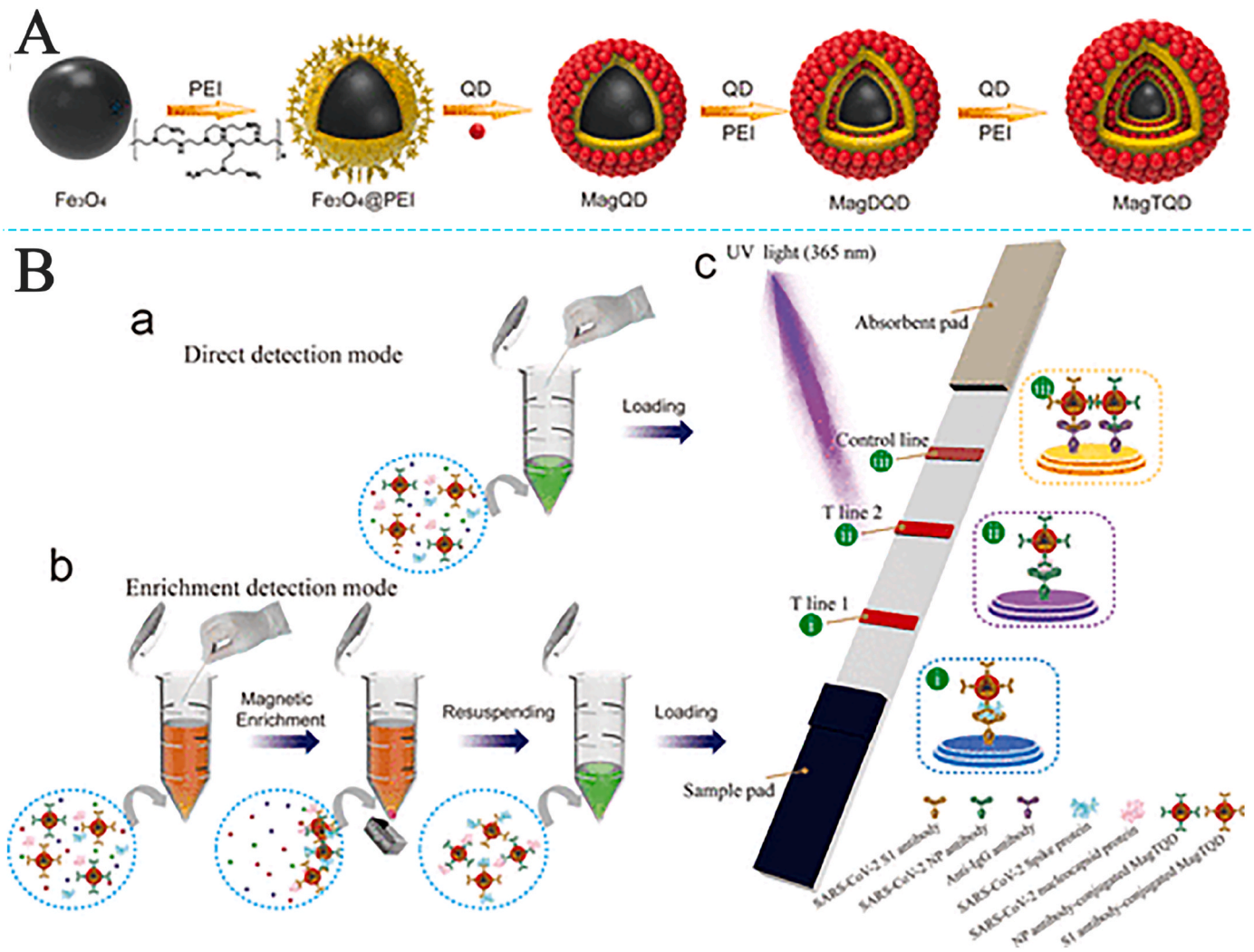

Fig. 8. Schematic of MagTQD preparation and detection process [103].

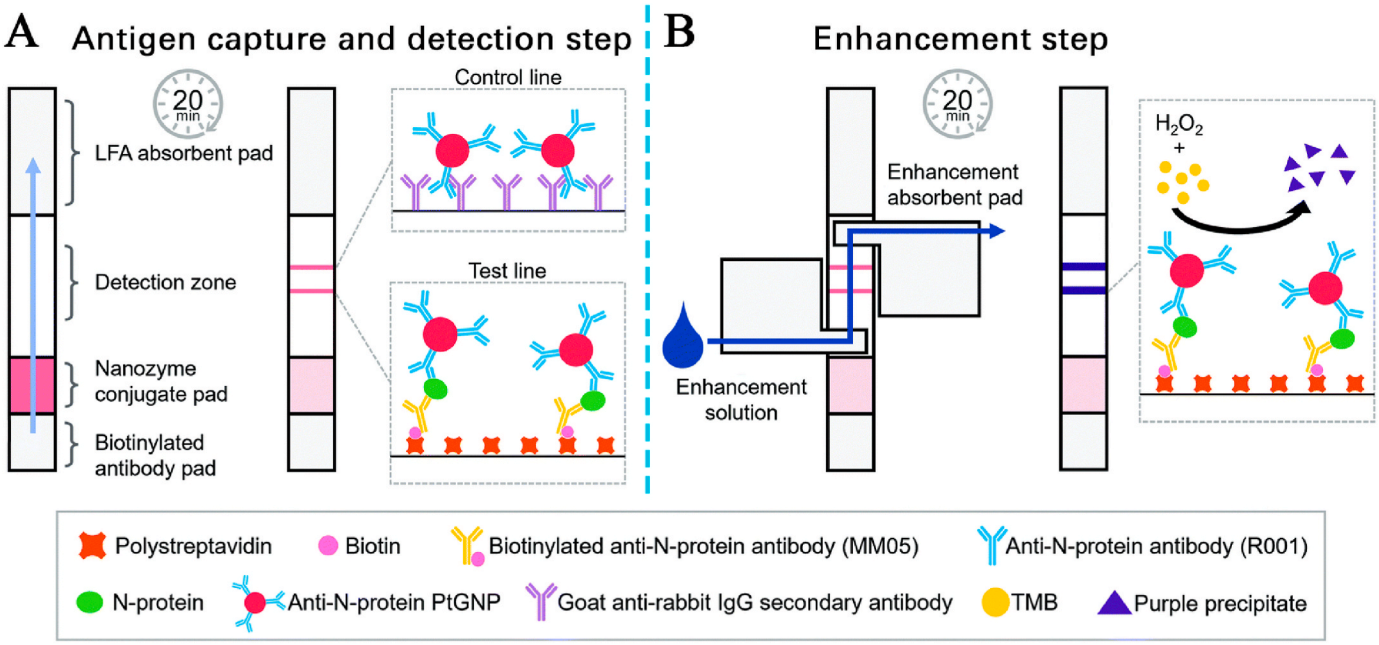

Fig. 9. Schematic of LFA and enhancement step [108].

The S protein is comprised of two subunits of N-terminal S1 and C-terminal S2 [117]. The N-terminal domain (NTD) and RBD are on the S1 subunit. They have the vital functions of recognizing sialic acid carbohydrate and binding to the angiotensin-converting enzyme 2 (ACE2) of the host cell, respectively [118,119]. The S2 subunit plays the part of changing conformation and inserting fusion peptide into the target cell membrane, resulting in viral entry [120]. The structural SARS-CoV-2 S protein is immunogenic, and can also be used for COVID-19 diagnosis, according to the WHO [99].

Han et al. [110] designed a colorimetric and fluorescent dual-functional LFA for sensitive detection of the S1 protein of SARS-CoV-2. Au NPs and carboxylate CdSe/ZnS quantum dots loaded on functional silica spheres (SiO_2@Au/QDs) provided colorimetric and fluorescent dual-signals. A schematic of material preparation and results of LFA fluorescence detection are shown in Fig. 10. The LODs were 1 and 0.033 ng/mL via colorimetry and fluorescence, respectively. Other researches focus on reducing the use of antibodies and designing new sandwich structures to capture and detect S protein. GiKim's team [114] developed a LFA based on angiotensin-converting enzyme 2 capturing SARS-CoV-2 S protein, in which red cellulose nanobeads were the signal source probed by a portable analyzer. The detection range was 5 ng/mL ~500 ng/mL. Baker et al. [111] found that α,N-acetyl neuraminic acid with affinity for the spike glycoprotein acted as a ligand. Based on this foundation, they designed glyco-Au NPs LFA to detect SARS-COV-2 S protein with a LOD of 5 μg/mL. Glycans conjugated on an Au NP modified with α-terminal thiol, by displacement of an ω-terminal pentafluorophenyl group, were called glyco-Au NPs. Kim et al. [112] utilized glycopolymers as primary capture and antibodies labeled with Au NPs as signal source to develop a LFA for detecting SARS-CoV-2 with a LOD of 3.13 μg/mL. A graphical illustration of virus interaction with glycosaminoglycans and LFA is shown in Fig. 11. Glycopolymers played an important role in binding the spike glycoprotein of SARS-CoV-2. Compared to current LFAs, this technology using one antibody lowered the cost, about 10-fold. Compared to the above study, an antibody-free LFA for detecting SARS-CoV-2 was fabricated by Pun's group [113]. Two DNA aptamers 1 (SNAP1) and 4 (SNAP4) were used to bind the SARS-CoV-2 S protein N-terminal domain, and SNAP4 conjugated Au NPs for colorimetric assay. The assay detects 250 pM SARS-CoV-2 S protein and UV-inactivated SARS-CoV-2 virus at 10^6 copies/mL.

The LFAs for N and S protein were summarized in Table 2 for scanning. N protein is more representative protein with stable structure and low mutation probability, which results in more researches about LFA for N protein, confirmed in Table 2. The number of studies on the detection of N protein by colorimetric and fluorescent LFA is comparable. In addition to colloidal gold, colored microspheres are also favored by researchers as signal markers for colorimetric LFA. The lowest detection limit of colorimetric LFA can reach 38 ng/mL. Quantum dots are commonly used in fluorescent LFA. The MagTQD-based LFA showed the best performance for simultaneous detection of N and S proteins, and the detection limit was as low as 0.5 pg/mL. It is believed that this will greatly encourage researchers to devote themselves to the research of fluorescent LFA sensitized by quantum dots. Without additional amplification greatly reduces the time required for field testing, which is most easily promoted as a means for rapid self-screening of large numbers of people.

3.4. LFA for antibodies for SARS-CoV-2 detection

The innate and adaptive immune response is triggered first in the event of the SARS-CoV-2 invasion. The phagocytosis of virus by macrophages is accelerated to slow viral spread [121]. T lymphocytes are activated that stimulate antibody and pro-inflammatory cytokine production from B and T cells, respectively [122]. NAs, IgM, IgG, and IgA against SARS-CoV-2 are produced in abundance. IgA antibody appears first after the infection in mouth, airway, tears, saliva, and breast milk [123]. It is significant for mucosal immunity [124], but is dominant only in the early stages of infection, thereafter decaying quickly [125]. Specific IgM antibody is found in the blood four days after SARS-CoV-2 infection, with a peak at about twenty days [126] and clears pathogens in the earliest stages. Detection of IgM can indicate a person suffering an acute infection or recently recovered [127]. IgG, as a main type of antibody, accounts for three-quarters of total blood immunoglobulin and appears shortly after IgM [121,128]. It can enter tissues to fight infection. NAs are a subset of antibodies, produced by B lymphocytes [129]. They can bind to S protein, or rather RBD of SARS-CoV-2 [130]. NAs may be IgG, IgM, IgA, *etc.* but not all IgG and IgM are NAs. Moreover, vaccination against SARS-CoV-2 also causes an immune response, and produces the corresponding antibodies [126].

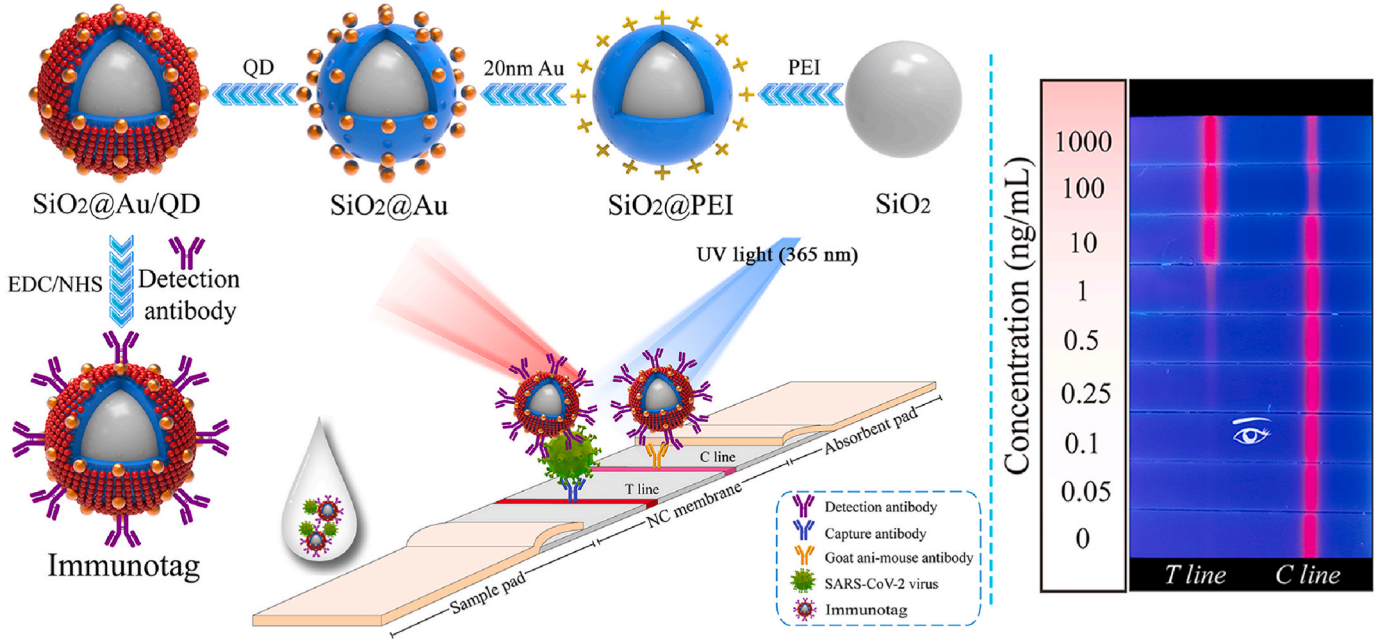

Fig. 10. Schematic of material preparation and results of fluorescence LFA (A) [110].

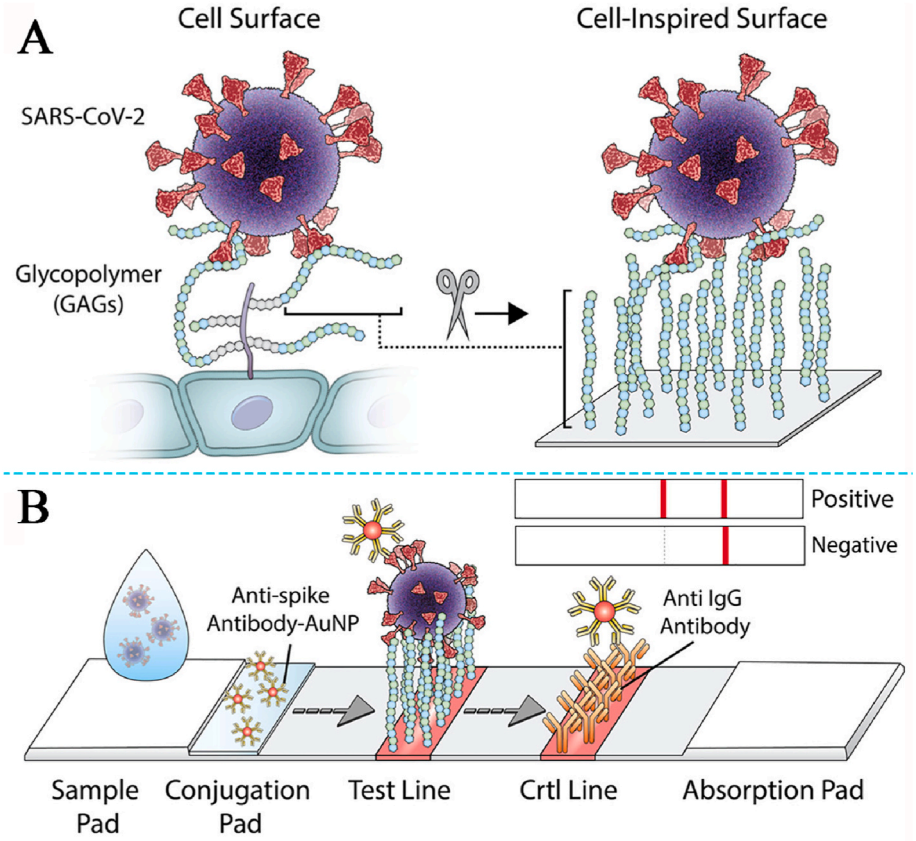

Fig. 11. Schematic of graphical illustration of virus interaction with glycosaminoglycans (A) and LFA (B) [112].

Table 2
LFA for N and S protein of SARS-CoV-2.

Target protein	Detection method	Signal material	Detection range (ng/mL)	LOD (ng/mL)	Reference
N	Colorimetry	Au NP clusters	0.030–1000	0.038	[100]
	Colorimetry	Red latex microspheres	25–5000	25	[101]
	Colorimetry	Red and blue latex beads	–	0.65	[107]
	Photothermal	Colored latex beads	0.2–100	0.13	[109]
	Nanozyme signal enhancement	Au@Pt NZs	0.1–1000	0.1	[108]
	Fluorescence	Carbon dots	0.010–1000	0.010	[102]
	Fluorescent or magnetic	A composite of Fe_3O_4 core with CdSe/ZnS QDs shells	0.05–500 or 0.5–1000	0.012 or 0.235	[104]
N or RBD	Fluorescence	AIE fluorescence molecule	1–20,000	7.2 or 6.9	[106]
N and S	Fluorescence	MagTQD	0.001–1000	0.0005	[103]
S	Colorimetry and fluorescence	SiO_2@Au/QDs	1–1000 and 0.1–1000	1 and 0.033	[110]
	Colorimetry	Glyco-Au NPs	–	5000	[111]
	Colorimetry	Au NPs	3130–50,000	3130	[112]
	Colorimetry	Au NPs	–	45	[113] [a]
S1	Colorimetry	Red cellulose nanobeads	50–1000	50	[114]

[a] The relative molecular weight of S protein was calculated as 190 kDa.

3.4.1. Colorimetric LFA

Wen et al. [131] designed a colloidal gold LFA for SARS-CoV-2 IgG with sensitivity of 69.1%. Jiao's team [132] also developed a colloidal gold LFA for SARS-CoV-2 IgM with sensitivity and specificity of 100% and 93.3%. Additionally, Zhou et al. [133] fabricated a gold nanoparticle-based LFA sensitized by polyethyleneimine-assisted copper in-situ growth. This assay not only had a low LOD of 50 fg/mL for HIV-1 capsid p24 antigen, but also showed a good performance in detecting SARS-CoV-2 antibody. These research efforts have played a certain role in promoting the development of LFA. Jabin's group [134] developed a LFA for anti-SARS-CoV-2 IgG based on silver NPs-Prot-S stabilized by calix [4]arene (Ag NPs-X_4-Prot-S) and Au NPs-citrate-Rabbit IgG. The synthesis of Ag NPs-X_4-Prot-S and LFA detection is displayed in Fig. 12. When the sample contained anti-SARS-CoV-2 IgG, the IgG-binding proteins at the T line captured the Ag NPs-X_4-Prot-S-antibody complexes, generating yellow color; red color was generated due to Au NPs-citrate-Rabbit IgG captured by anti-Rabbit IgG on the C line. It showed low LODs of 5 ng/mL and a sensitivity of 73% for Anti-SARS-CoV-2 IgG in buffer. The strategy of stabilizing silver can broaden the application of silver nanoparticles, which is conducive to promoting the application of new materials in colorimetric LFA.

Diani et al. [135] performed an analysis of COVID-19 IgG/IgM in blood rapid test colloidal gold LFIA (Menarini, Florence, Italy). Interestingly, the assay showed higher sensitivity of 91.49% after 10 days from symptom onset. Black et al. [136] used a commercial colloidal gold FLA of Biolidics 2019-nCoV IgG/IgM Detection Kit to detect anti-SARS-CoV-2 IgM and IgG. Its clinical sensitivity was 92%. These studies indicate good performance and utility for clinical detection. Thus, improving its sensitization has great significance. Li et al. [137] developed a triple-line colloidal gold LFA for simultaneously detecting SARS-CoV-2 IgM and IgG in human blood. It had a sensitivity and specificity of 88.66% and 90.63%, respectively. Coincidentally, Zeng

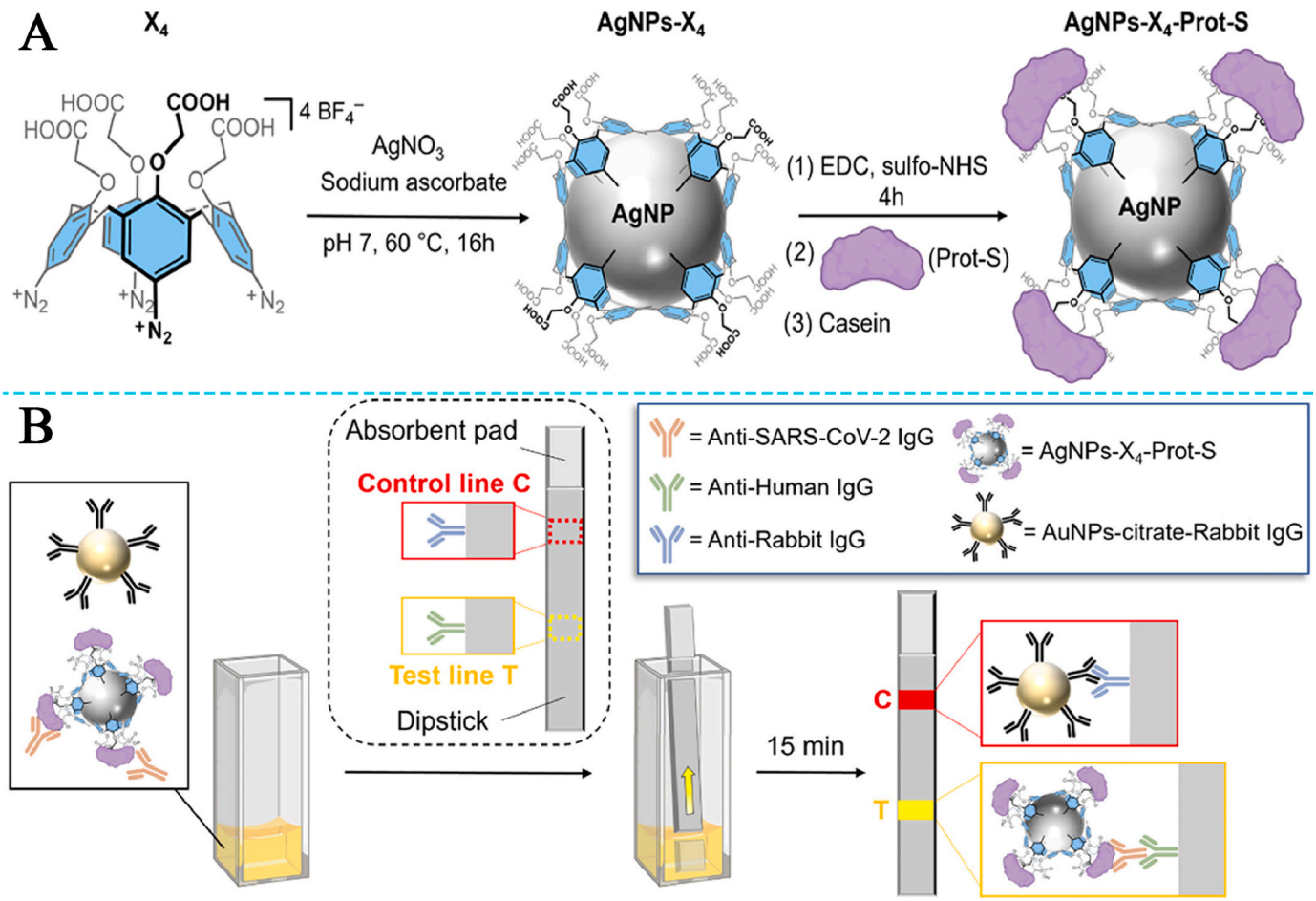

Fig. 12. Schematic of the synthesis of AgNPs-X_4-Prot-S (A) and LFA detection (B) [134].

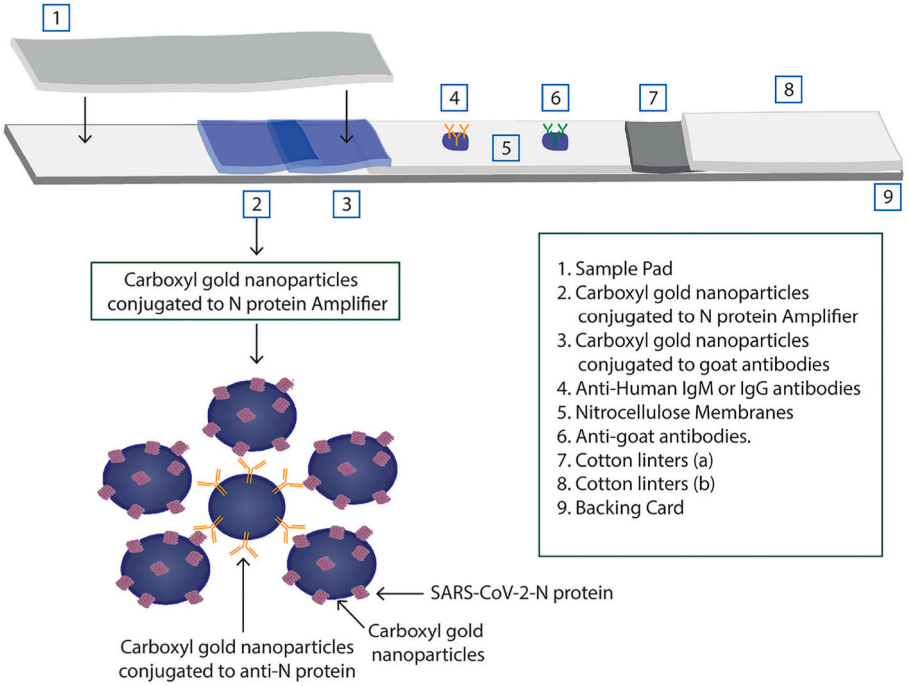

Fig. 13. Schematic of the LFA and the amplifier conjugate [140].

et al. [138] also reported a similar colloidal gold LFA that had a positive rate of 85.29% combining IgG-IgM. Additionally, Liu et al. [139] used a similar colloidal gold LFA for IgM and IgG. Alhabbab et al. [140] developed a LFA to detect IgM or IgG antibodies based on the signal amplification platform of a complex. The complex was an Au NP conjugated antibody integrating five Au NPs conjugated by SARS-CoV-2 N proteins. Its structure is shown in Fig. 13. It has a sensitivity of 94% or 96% and seen visually LOD of 0.55 or 0.4 by optical density for SARS-CoV-2 N protein IgM and IgG antibodies, respectively. Wang et al. [141] fabricated a triple-line FLA for detecting SARS-CoV-2 IgM and IgG based on selenium nanoparticles. The assay had a LOD of 20 ng/mL and 5 ng/mL read by the naked eye and a sensitivity and specificity of 93.33% and 97.34%, respectively.

3.4.2. *Fluorescent LFA*

Chen et al. [142] designed a fluorescent LFA for anti-SARS-CoV-2 IgG based on lanthanide (Eu)-doped polysterene nanoparticles. Due to limits of anti-SARS-CoV-2 IgG, this assay can only be tested semi-quantitatively. Significantly, ratiometric fluorescent analysis was first applied to fluorescent LFAs by Duan's group [143]. This LFA for NAb employed carboxyl-functionalized Europium chelate nanoparticles (Eu NPs) as the signal source. The Eu NP conjugated chicken IgY antigens (IgY-EuNPs) as a standardized reference were captured by anti-chicken IgY (anti-IgY) on the C line. The signals of T1 and T2 lines from the Eu NPs conjugated SARS CoV-2 RBD (RBD-EuNPs) appeared as two reverse response signals. Its detection schematic is exhibited in Fig. 14. The linearity range was 12.5–1000 IU/mL and LOD was 7.6 IU/mL. This strategy opens a new idea for the research on LFA.

Wang et al. [144] applied silica-core@CdSe/ZnS QDs shell nanocomposites to develop a fluorescent FLA for simultaneous detection of SARS-CoV-2-specific IgM and IgG. Its sensitivity and specificity reached 97.37% and 95.54%. Jia et al. [145] prepared silica enriched and encapsulated CdSe/CdS/ZnS QDs composites, aimed at developing to a fluorescent FLA for detecting SARS-CoV-2 IgG, IgM, or IgA, respectively. The assay showed low LODs for SARS-CoV-2 IgG (0.10 ng/mL), IgM (0.04 ng/mL), or IgA (0.06 ng/mL), with sensitivity and specificity reaching 100%, and the accuracy of 97.15%. The AIE nanoparticles were also utilized in fluorescent FLA for SARS-CoV-2 antibodies. Chen et al. [146] used 4,8-bis(4-(2,2-bis(4(octyloxy)phenyl)-1-phenylvinyl) phenyl)benzo[1,2-*c*:4,5-*c*′]bis [1,2,5]thiadiazole as the fluorescent unit to prepared AIE nanoparticles. They developed a fluorescent LFA based on AIE nanoparticles for simultaneous detection of IgM and IgG with 100% specificity and accuracy, respectively. The synthesis of AIE nanoparticles and LFA for IgM and IgG is represented in Fig. 15. The LODs were 0.236 μg/mL and 0.125 μg/mL for IgM and IgG.

Wang et al. [147] synthesized fluorescent polymeric nanoparticle based AIE luminogens and used them to fabricate a triple-line fluorescent FLA for detecting SARS-CoV-2 IgM and IgG. Li's team [148] reported a triple-line fluorescent FLA for simultaneous detection of SARS-CoV-2 IgM and NAb based on polystyrene-coated quantum dot nanoparticles. It displayed a sensitivity of 90.0% and 82.9% for IgM and Nab. Compared with IgM or IgG, total antibodies are considered as the

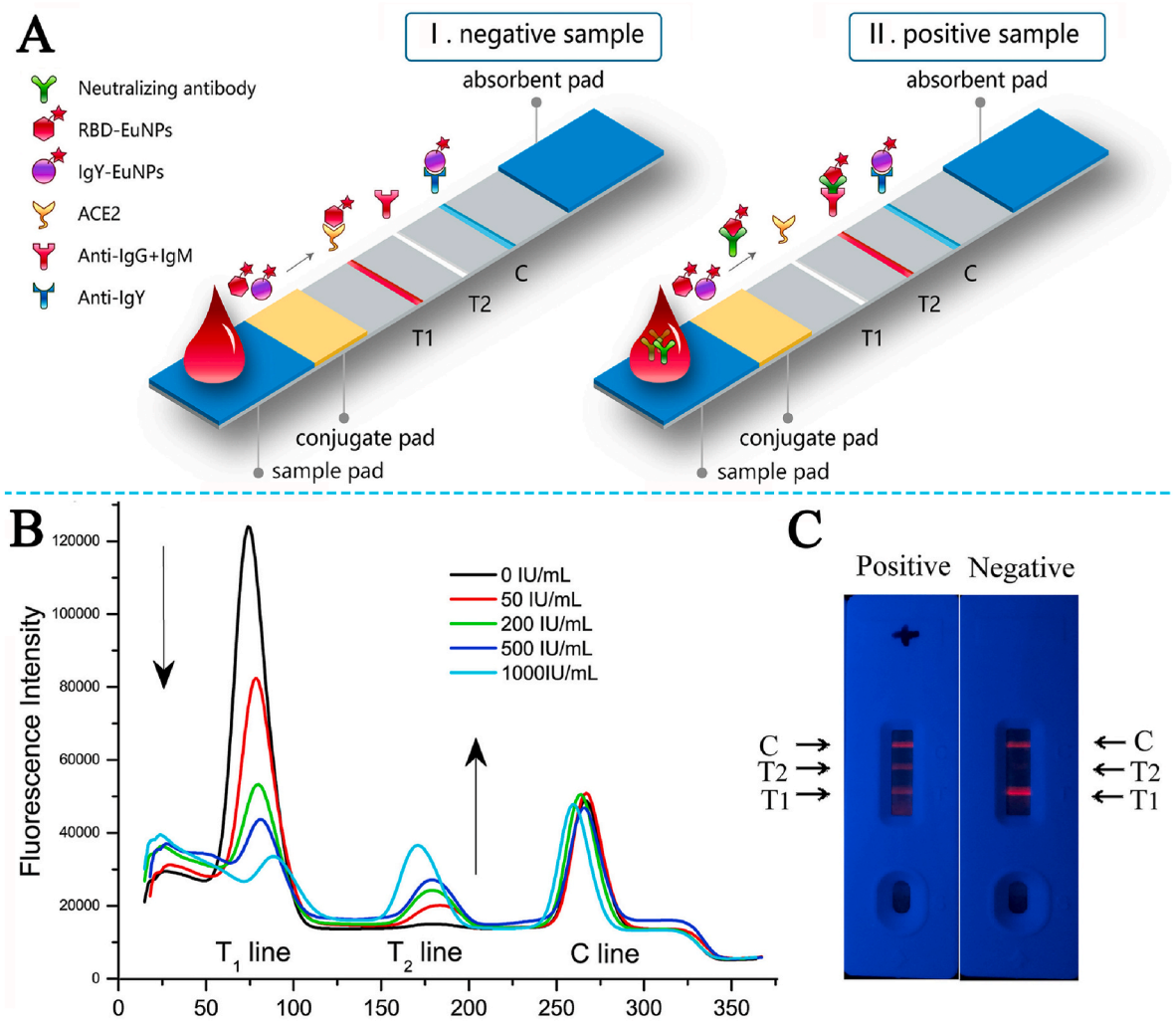

Fig. 14. Schematic of the LFA (A) and detection results (B, C) [143].

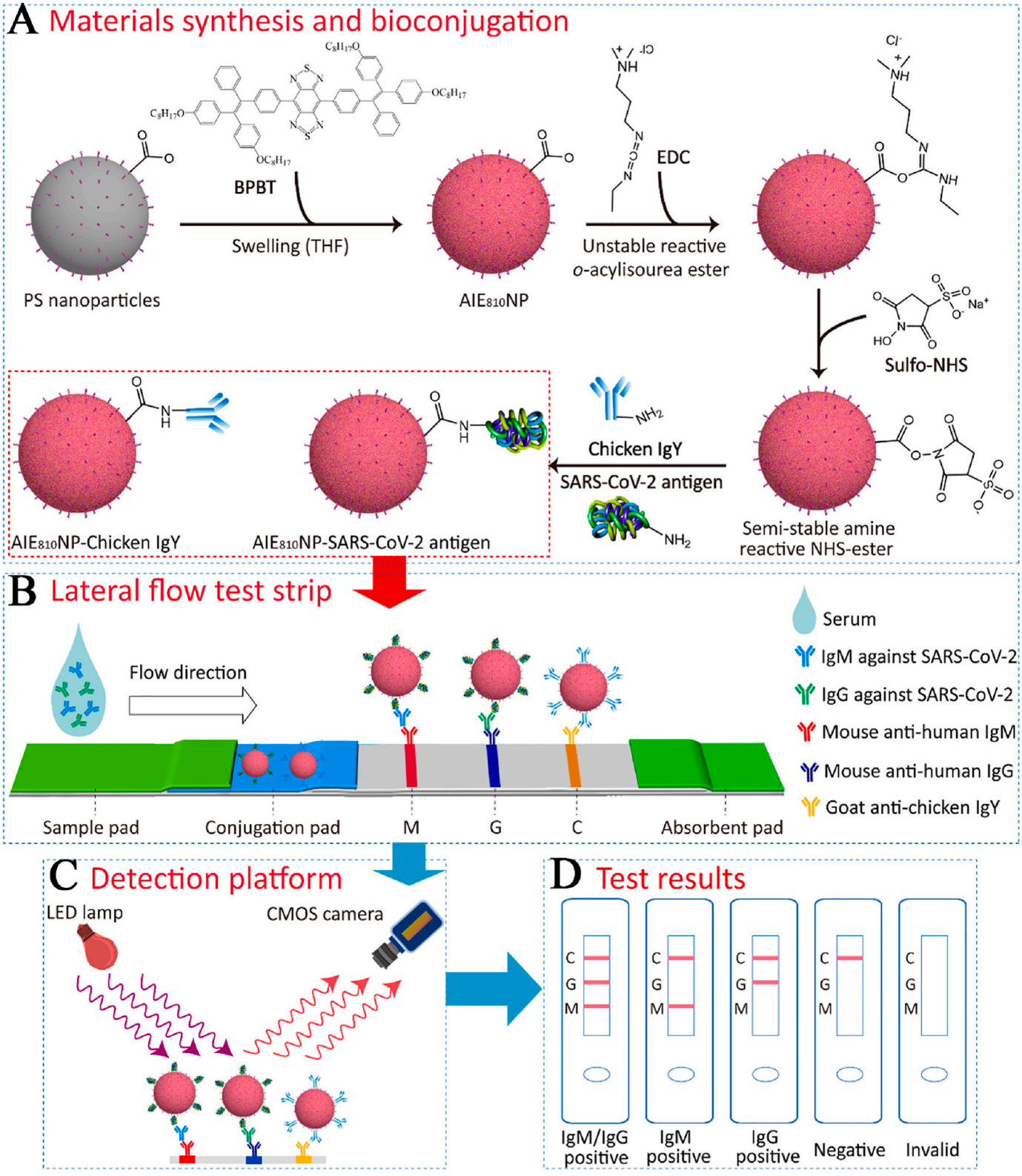

Fig. 15. Schematic of the AIE nanoparticle-labeled LFA [146].

more sensitive and earlier serological marker, and recommended as a diagnostic standard for COVID-19 by the WHO. Zhou et al. [149] used octadecylamine coated CdSe/ZnS QDs as signal source to design a fluorescent FLA for SARS-CoV-2 total antibodies. The assay displayed high sensitivity, specificity, and accuracy of 97.1%, 100%, and 95%. Similarly, Xu's group [150] reported a colloidal gold LFA for SARS-CoV-2 total antibodies with a specificity of 100%.

3.4.3. CL, SERS, and magnetic LFA

Roda et al. [151] developed a dual-signal of colorimetric and CL LFA to determine SARS-CoV-2 IgA. The colorimetric and CL signal originated from Au NPs and luminol/H_2O_2 catalyzed via horseradish peroxidase,

respectively. The assay showed sufficient sensitivity and reproducibility for the semi-quantification of IgA. Liu et al. [152] fabricated a SERS-based LFA for anti-SARS-CoV-2 IgM/IgG based on signal materials with core-shell structure labeled with dual layers of Raman dye easily recorded by a portable Raman instrument. The tag was a SiO_2 core multilayered shell of Au-seed NPs labeled with DTNB and Ag NPs labeled with DTNB (Dual-layers DTNB-modified SiO_2@Ag), displayed a good SERS signal and stability. A schematic of the LFA is vividly presented in Fig. 16. The LODs were 1.28×10^7-fold dilution by the IUPAC standard method, 800 times lower than that of the visualization results. The assay exhibited 100% accuracy and specificity for anti-SARS-CoV-2 IgM/IgG, and provided an efficient supplementary means. Chen's group [153] designed a triple-line SERS-based LFA for simultaneous detection of SARS-CoV-2 IgM and IgG. Au NPs modified with 4-nitrobenzenethiol acted as signal source. It possessed high specificity and accuracy (100%), and LODs were 1 ng/mL and 0.1 ng/mL for IgM and IgG, respectively. Srivastav et al. [154] developed a SERS-based LFA for SARS-CoV-2-specific IgM/IgG based on Au nanostars labeled with NIR-797-isothiocyanate. The assay had a low LOD of 100 fg/mL seven orders of magnitude lower than the detection by naked-eye. In addition, a giant magnetoresistance based LFA for IgM and IgG simultaneously based on superparamagnetic nanoparticles was reported Guo's team [155]. The superparamagnetic nanoparticles had an average diameter of 68 nm with good dispersibility and magnetic properties and were synthesized by a simple and time-effective co-precipitation method. Quantitative ranges of 10–250 ng/mL and 5–250 ng/mL for IgM and IgG were shown with LODs of 10 ng/mL and 5 ng/mL, respectively. These detection methods enrich LFAs and promote the research of multi-signal detection, and provide multiple directions for the subsequent development of LFA.

The above reports on antibodies detection by LFA are summarized in Table 3. Because antibodies appear relatively late in infected people, LFA testing for antibodies is generally used as a post-cure observation. According to the above reports, although the quantitative detection of colorimetric LFA is difficult, its sensitivity and specificity can meet the detection requirements without the need for expensive and specialized instruments. Importantly, the simple operation and output mode (visible to the naked eye) has facilitated its use in a large number of screening, outdoor and self-testing applications. Compared with the colorimetric method, the fluorescence and Raman output modes can realize the quantitative detection of LFA, and achieve a lower detection limit. However, its materials used as signal markers are more complex than the preparation of colloidal gold, and the detection equipment is more expensive, which is generally used in laboratory testing.

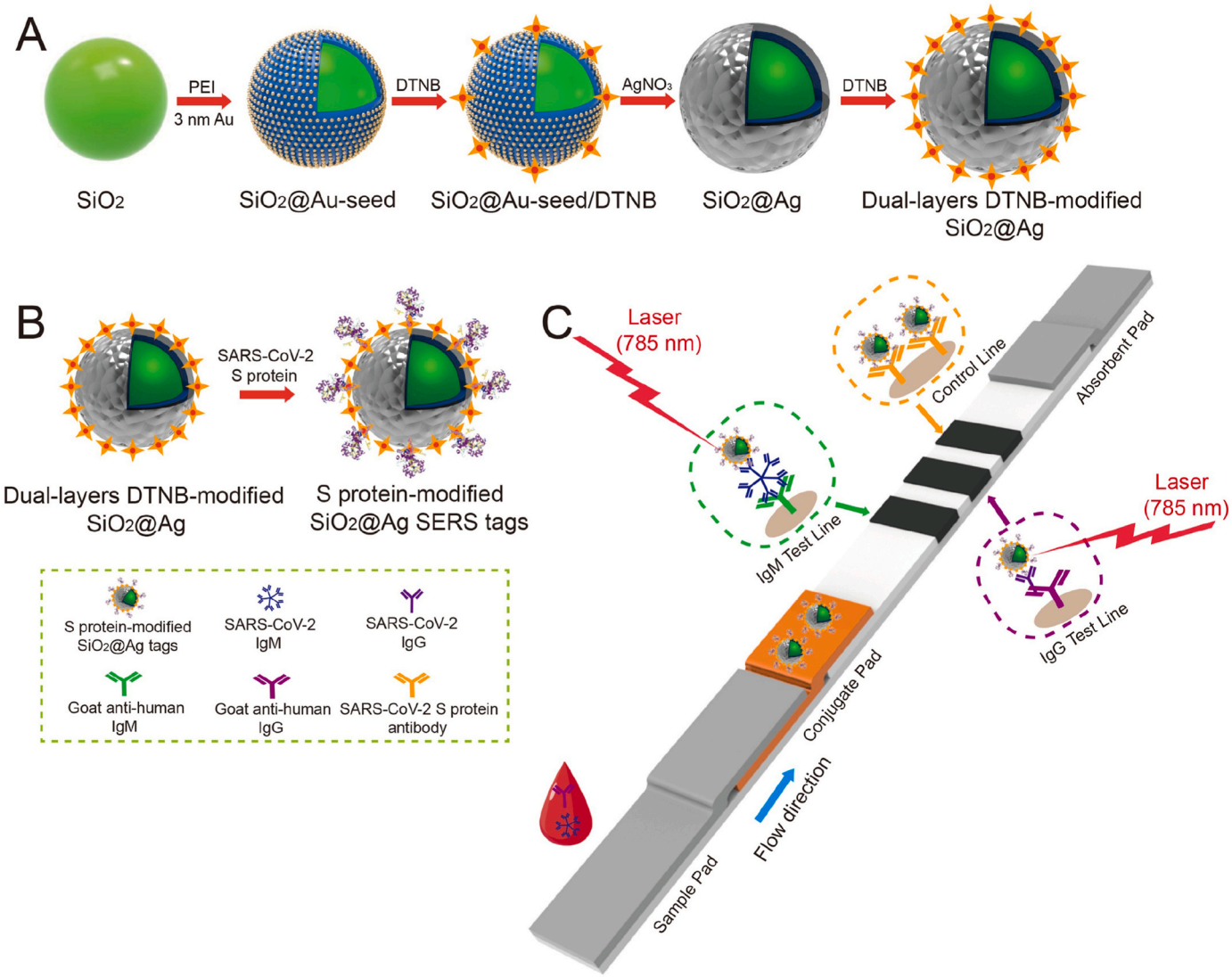

Fig. 16. Schematic of the preparation of the signal material (A), S protein-modified signal material SERS tags (B), and SERS-LFIA strip (C) [152].

Table 3
LFA for N and S protein of SARS-CoV-2.

Detection method	Target	Signal source	Detection range	LOD	Sensitivity (%)	Specificity (%)	Reference
Colorimetry	IgG	Au NPs	–	–	69.1		[131]
	IgM	Au NPs	–	–	100	93.3	[132]
	Antibody	Polyethyleneimine-assisted copper growing on Au NPs	–	–	89.9	–	[133]
	IgG	Ag NPs-X_4-Prot-S	–	5 ng/mL	73	100	[134]
	IgG/IgM	Au NPs	–	–	91.49	100	[135]
	IgG/IgM	Au NPs	–	–	92	100/92	[136]
	IgM and IgG	Au NPs	–	–	88.66	90.63	[137]
	IgG and IgM	Au NPs	–	–	85.29	100	[138]
	IgM and IgG	Au NPs	–	–	–	–	[139]
	IgM or IgG	A complex formed by six Au NPs	0.55–1 or 0.4–1 optical density	0.55 or 0.4 optical density	94 or 96	93 or 98	[140]
	IgM and IgG	Selenium nanoparticles	20–200 and 5–200 ng/mL	20 and 5 ng/mL	93.33	97.34	[141]
Fluorescence	Anti-SARV-CoV-2 IgG	Eu-doped polysterene nanoparticles	–	–	–	–	[142]
	NAb	Eu NPs	12.5–1000 IU/mL	7.6 IU/mL	–	–	[143]
	IgM and IgG	silica-core@CdSe/ZnS QDs shell nanocomposites	0.1–0.000001 dilution	0.0000001 dilution	97.37	95.54	[144]
	IgG, IgM, or IgA	CdSe/CdS/ZnS QDs	0.10–1,000, 0.04–1,000, or 0.06–1000 ng/mL	0.10, 0.04, or 0.06 ng/mL	–	100	[145]
	IgM and IgG	AIE nanoparticles	313–5,000, 156–5000 ng/mL	236 and 125 ng/mL	78 and 95	–	[146]
	IgM and IgG	Polymeric nanoparticles	–	–	–	–	[147]
	IgM and NAb	polystyrene-coated Quantum dot nanoparticles	–	–	90.0 and 82.9	100	[148]
	Total antibodies	octadecylamine coated CdSe/ZnS QDs	–	–	97.1	100	[149]
	Total antibodies	Au NPs	–	–	–	100	[150]
Colorimetry and CL	IgA	Au NPs and luminol/H_2O_2 horseradish peroxidase	–	–	–	–	[151]
SERS	anti-SARS-CoV-2 IgM/IgG	Dual-layers DTNB-modified SiO_2@Ag	1000–12,800,000-fold dilution	12,800,000-fold dilution	–	100	[152]
	IgM and IgG	Au NPs modified with 4-nitrobenzenethiol acted	1–1,000, 0.1–1000 ng/mL	1 and 0.1 ng/mL	–	–	[153]
	IgM/IgG	Au nanostars labeled with NIR-797-isothiocyanate	0.0001–1000 ng/mL	0.0001 pg/mL	–	–	[154]
Magnetic	IgM and IgG	Superparamagnetic nanoparticles	10–250 and 5–250 ng/mL	10 and 5 ng/mL	–	–	[155]

4. Conclusions and future perspectives

The diagnosis of SARS-CoV-2 at an early stage identifies SARS-CoV-2-infected persons which is conducive to controlling the spread and resurgence of COVID-19. In this aspect, LFA detection plays a crucial part in targeting SARS-CoV-2 specific biomarkers, for instance genes, N protein, S protein, and antibodies. Due to their fast, portable, low cost, and user friendly natures, various LFA platforms have sprung up. This review provided an overview of the sandwich mode LFA techniques for SARS-CoV-2 diagnosis. We classify research according to the target (genes, N protein, S protein, and antibodies) and different signal detection types. Furthermore, the properties of the targets were introduced to clarify their detection significance. Reviewed all the study, colloidal gold colorimetric LFA studies occupied the largest number in nucleic acid, protein, antibody detection. The application of Dye streptavidin coated polymer nanoparticles, red cellulose nanobeads and other materials has also promoted the development of colorimetric LFA. Fluorescence and Raman can detect the accumulation of material on the T line that is not visible to the naked eye, greatly improving the sensitivity of detection. Quantum dots are the main materials applied to the sensitization of fluorescent LFA and also shows attractive performance. LFA sensitization using novel materials has always played an important role in research. In addition to material sensitization strategy, gene amplification is also an important sensitization method for LFA detecting nucleic acid. In the LFA for protein detection, there are also many studies on using different capture methods to efficiently identify target detection proteins.

Although LFA research is extensive and commercial products for SARS-CoV-2 detection are also manufactured, challenges remain. I) The detection limit of fluorescence and Raman LFA can reach the level of pg/mL [103], but further sensitization to achieve high signal response changes caused by small concentration of target substances is still the goal of researchers. II) Generally speaking, the limited information obtained by the analysis in complex samples via single target and single signal detection mode is insufficient [10]. III) Laboratory self-made portable testing equipment without unified standardization is not conducive to mass production and popularization. IV) The mutation of SARS-CoV-2 protein and nucleic acid makes it difficult to achieve the ideal detection effect of LFA constructed with pre-mutation specific antibody and aptamer. In view of the challenges, we propose the following four strategies. I) The preparation of label materials with high response signal, and high-resolution instrumentation to sensitize LFAs. II) Development of multiplexed type, multi-line type, and multi-signal type for multi-signal synchronous detection reduces the false positives [156]. III) Improving standardization and universality enhance the versatility of homemade portable devices and the comparability of test results between different homemade devices. IV) Simultaneous detection of multiple markers and timely selection of new immune targets in developing LFAs reduce false negatives caused by mutations.

The preparation of magnetic fluorescent materials, magnetic nanoenzyme materials and other composite materials has greatly promoted the development of dual signal detection mode of LFA [157]. The commercialization of micro/nanomaterials such as gold nanoparticles, magnetic microspheres and quantum dots has promoted the mass commercial production of LFA. Research on smartphone platform is promoting the LFA towards intelligent and digital detection, which will greatly facilitate the statistics of screening results and the management of health records [158,159]. The emergence of wearable LFA reduces

the sampling limitations [160]. Those techniques or materials greatly boost the research in LFA of COVID-19 detection. It is believed that with the development of science and technology, LFAs with high sensitivity, high accuracy, and universality for detecting SARS-CoV-2 will promote victory in the battle against COVID-19.

Declaration of competing interest

The authors declare that they have no known competing financial interests or personal relationships that could have appeared to influence the work reported in this paper.

Data availability

The authors do not have permission to share data.

Acknowledgments

The work was supported by the Foundationof State Key Laboratory of NBC Protection for Civilian(No. SKLNBC2019-05), and the National Natural Science Foundation of China (No. 51872140).

References

[1] J.L. Krleza, R.Z. Topic, V. Stevanovic, A. Lukic-Grlic, I. Tabain, Z. Misak, G. Roic, B. Kaic, D. Mayer, Z. Hruskar, L. Barbic, T. Vilibic-Cavlek, Seroprevalence of SARS-CoV-2 infection among children in Children's Hospital Zagreb during the initial and second wave of COVID-19 pandemic in Croatia, Biochem. Med. 31 (2) (2021) 12.
[2] H.P. Yao, Y.T. Song, Y. Chen, N.P. Wu, J.L. Xu, C.J. Sun, J.X. Zhang, T.H. Weng, Z.Y. Zhang, Z.G. Wu, L.F. Cheng, D.R. Shi, X.Y. Lu, J.L. Lei, M. Crispin, Y.G. Shi, L. J. Li, S. Li, Molecular architecture of the SARS-CoV-2 virus, Cell 183 (3) (2020) 730–738. E13.
[3] X. Liu, C. Liu, G. Liu, W.X. Luo, N.S. Xia, COVID-19: progress in diagnostics, therapy and vaccination, Theranostics 10 (17) (2020) 7821–7835.
[4] E.N. Nikolaev, M.I. Indeykina, A.G. Brzhozovskiy, A.E. Bugrova, A.S. Kononikhin, N.L. Starodubtseva, E.V. Petrotchenko, G.I. Kovalev, C.H. Borchers, G.T. Sukhikh, Mass-spectrometric detection of SARS-CoV-2 virus in scrapings of the epithelium of the nasopharynx of infected patients via nucleocapsid N protein, J. Proteome Res. 19 (11) (2020) 4393–4397.
[5] M. Asif, M. Ajmal, G. Ashraf, N. Muhammad, A. Aziz, T. Iftikhar, J.L. Wang, H. F. Liu, The role of biosensors in coronavirus disease-2019 outbreak, Curr. Opin. Electrochem. 23 (2020) 174–184.
[6] H.F. El Sharif, S.R. Dennison, M. Tully, S. Crossley, W. Mwangi, D. Bailey, S. P. Graham, S.M. Reddy, Evaluation of electropolymerized molecularly imprinted polymers (E-MIPs) on disposable electrodes for detection of SARS-CoV-2 in saliva, Anal. Chim. Acta 1206 (2022) 11.
[7] Z.T. Zhong, L.B. Song, C.Q. Li, X. Sun, W. Chen, B. Liu, Y.D. Zhao, Lateral flow biosensor for universal detection of various targets based on hybridization chain reaction amplification strategy with pregnancy test strip, Sens. Actuator B-Chem. 337 (2021) 12.
[8] X.R. Chen, L. Ding, X.L. Huang, Y.H. Xiong, Tailoring noble metal nanoparticle designs to enable sensitive lateral flow immunoassay, Theranostics 12 (2) (2022) 574–602.
[9] L. Huang, S.L. Tian, W.H. Zhao, K. Liu, X. Ma, J.H. Guo, Aptamer-based lateral flow assay on-site biosensors, Biosens. Bioelectron. 186 (2021) 13.
[10] Q. Zhang, L. Fang, B.Y. Jia, N. Long, L.C. Shi, L.D. Zhou, H.P. Zhao, W.J. Kong, Optical lateral flow test strip biosensors for pesticides: recent advances and future trends, Trac. Trends Anal. Chem. 144 (2021) 17.
[11] B. Perez-Lopez, M. Mir, Commercialized diagnostic technologies to combat SARS-CoV2: advantages and disadvantages, Talanta 225 (2021) 14.
[12] E. Ernst, P. Wolfe, C. Stahura, K.A. Edwards, Technical considerations to development of serological tests for SARS-CoV-2, Talanta 224 (2021) 13.
[13] L.Z. Chen, G.L. Zhang, L.Q. Liu, Z.D. Li, Emerging biosensing technologies for improved diagnostics of COVID-19 and future pandemics, Talanta 225 (2021) 10.
[14] G.-P. Dong, X.-J. Guo, Y.-A. Sun, Z. Zhang, L.-P. Du, M.-Y. Li, Diagnostic techniques for COVID-19: a mini-review of early diagnostic methods, J. Anal. Test. 5 (4) (2021) 314–326.
[15] A. Bisht, A. Mishra, H. Bisht, R.M. Tripathi, Nanomaterial based biosensors for detection of viruses including SARS-CoV-2: a review, J. Anal. Test. 5 (4) (2021) 327–340.
[16] J.Q. Bu, Z.W. Deng, H. Liu, J.C. Li, D. Wang, Y.J. Yang, S.A. Zhong, Current methods and prospects of coronavirus detection, Talanta 225 (2021) 14.
[17] Y.F. Zhou, Y.H. Wu, L. Ding, X.L. Huang, Y.H. Xiong, Point-of-care COVID-19 diagnostics powered by lateral flow assay, Trac. Trends Anal. Chem. 145 (2021) 15.
[18] N.S. Castrejon-Jimenez, B.E. Garcia-Perez, N.E. Reyes-Rodriguez, V. Vega-Sanchez, V.M. Martinez-Juarez, J.C. Hernandez-Gonzalez, Challenges in the detection of SARS-CoV-2: evolution of the lateral flow immunoassay as a valuable tool for viral diagnosis, Biosens. Bioelectron. 12 (9) (2022) 18.
[19] R. Bucci, D. Maggioni, S. Locarno, A.M. Ferretti, M.L. Gelmi, S. Pellegrino, Exploiting ultrashort alpha,beta-peptides in the colloidal stabilization of gold nanoparticles, Langmuir 37 (38) (2021) 11365–11373.
[20] V. Ranganathan, S. Srinivasan, A. Singh, M.C. DeRosa, An aptamer-based colorimetric lateral flow assay for the detection of human epidermal growth factor receptor 2 (HER2), Anal. Biochem. 588 (2020) 10.
[21] L.H. Su, H.L. Hu, Y.L. Tian, C.H. Jia, L.L. Wang, H. Zhang, J.L. Wang, D.H. Zhang, Highly sensitive colorimetric/surface-enhanced Raman spectroscopy immunoassay relying on a metallic core-shell Au/Au nanostar with clenbuterol as a target analyte, Anal. Chem. 93 (23) (2021) 8362–8369.
[22] M.S. Khan, H. Ameer, Y.W. Chi, Label-free and ultrasensitive electrochemiluminescent immunosensor based on novel luminophores of Ce2Sn2O7 nanocubes, Anal. Chem. 93 (7) (2021) 3618–3625.
[23] S. Song, S. Choi, S. Ryu, S. Kim, T. Kim, J. Shin, H.I. Jung, C. Joo, Highly sensitive paper-based immunoassay using photothermal laser speckle imaging, Biosens. Bioelectron. 117 (2018) 385–391.
[24] Z. Chen, Z.Y. Zhang, J. Qi, J.M. You, J.P. Ma, L.X. Chen, Colorimetric detection of heavy metal ions with various chromogenic materials: strategies and applications, J. Hazard Mater. 441 (2022) 20.
[25] G.A. Zhao, S.J. Liu, L. Guo, W.T. Fang, Y.J. Liao, L. Rui, L.S. Fu, J.L. Wang, A customizable automated container-free multi-strip detection and line recognition system for colorimetric analysis with lateral flow immunoassay for lean meat powder based on machine vision and smartphone, Talanta 253 (2022) 8.
[26] X. Yan, H.X. Li, X.G. Su, Review of optical sensors for pesticides, Trac. Trends Anal. Chem. 103 (2018) 1–20.
[27] C. Schmidt, H. Borcherding, T. Thiele, U. Schedler, F. Werner, S. Rodiger, D. Roggenbuck, P. Schierack, Fluorescence-encoded poly(methyl metharcylate) nanoparticles for a lateral flow assay detecting IgM autoantibodies in rheumatoid arthritis, Anal. Biochem. 633 (2021) 7.
[28] M. Ali, M. Sajid, M.A.U. Khalid, S.W. Kim, J.H. Lim, D. Huh, K.H. Choi, A fluorescent lateral flow biosensor for the quantitative detection of Vaspin using upconverting nanoparticles, Spectroc. Acta Pt. A-Molec. Biomolec. Spectr. 226 (2020) 9.
[29] F.L. He, X.F. Lv, X.Q. Li, M.D. Yao, K.J. Li, Y.L. Deng, Fluorescent microspheres lateral flow assay integrated with Smartphone-based reader for multiple microRNAs detection, Microchem. J. 179 (2022) 13.
[30] Y. Pang, Q. Li, C. Wang, S. Zhen, Z. Sun, R. Xiao, CRISPR-cas12a mediated SERS lateral flow assay for amplification-free detection of double-stranded DNA and single-base mutation, Chem. Eng. J. 429 (2022) 9.
[31] X.F. Jia, K.L. Wang, X.Y. Li, Z.Z. Liu, Y. Liu, R. Xiao, S.Q. Wang, Highly sensitive detection of three protein toxins via SERS-lateral flow immunoassay based on SiO_2@Au nanoparticles, Nanomed. Nanotechnol. Biol. Med. 41 (2022) 11.
[32] H.Y. Yang, Q.Y. He, M.X. Lin, L. Ji, L.H. Zhang, H.X. Xiao, S.J. Li, Q.L. Li, X.P. Cui, S.Q. Zhao, Multifunctional Au@Pt@Ag NPs with color-photothermal-Raman properties for multimodal lateral flow immunoassay, J. Hazard Mater. 435 (2022), 129082.
[33] C.W. Wang, C.G. Wang, X.L. Wang, K.L. Wang, Y.H. Zhu, Z. Rong, W.Y. Wang, R. Xiao, S.Q. Wang, Magnetic SERS strip for sensitive and simultaneous detection of respiratory viruses, ACS Appl. Mater. Interfaces 11 (21) (2019) 19495–19505.
[34] X.X. Liu, X.S. Yang, K. Li, H.F. Liu, R. Xiao, W.Y. Wang, C.W. Wang, S.Q. Wang, Fe3O4@Au SERS tags-based lateral flow assay for simultaneous detection of serum amyloid A and C-reactive protein in unprocessed blood sample, Sens. Actuator B-Chem. 320 (2020) 10.
[35] Y. Zeng, K.M. Koo, M. Trau, A.G. Shen, J.M. Hu, Watching SERS glow for multiplex biomolecular analysis in the clinic: a review, Appl. Mater. Today 15 (2019) 431–444.
[36] D. Zhang, L. Huang, B. Liu, H.B. Ni, L.D. Sun, E.B. Su, H.Y. Chen, Z.Z. Gu, X. W. Zhao, Quantitative and ultrasensitive detection of multiplex cardiac biomarkers in lateral flow assay with core-shell SERS nanotags, Biosens. Bioelectron. 106 (2018) 204–211.
[37] H.C. Shen, K.X. Xie, L.P. Huang, L. Wang, J.H. Ye, M. Xiao, L. Ma, A.Q. Jia, Y. Tang, A novel SERS-based lateral flow assay for differential diagnosis of wild-type pseudorabies virus and gE-deleted vaccine, Sens. Actuator B-Chem. 282 (2019) 152–157.
[38] T. Wang, Z. Yang, C. Lei, J. Lei, Y. Zhou, An integrated giant magnetoimpedance biosensor for detection of biomarker, Biosens. Bioelectron. 58 (2014) 338–344.
[39] X.H. Mu, H.F. Liu, Z.Y. Tong, B. Du, S. Liu, B. Liu, Z.W. Liu, C. Gao, J. Wang, H. Dong, A new rapid detection method for ricin based on tunneling magnetoresistance biosensor, Sens. Actuator B-Chem. 284 (2019) 638–649.
[40] W. Wang, Y. Wang, L. Tu, T. Klein, Y.L. Feng, Q. Li, J.P. Wang, Magnetic detection of mercuric ion using giant magnetoresistance-based biosensing system, Anal. Chem. 86 (8) (2014) 3712–3716.
[41] J. Zhang, L.M. Tang, Q.C. Yu, W.W. Qiu, K. Li, L.L. Cheng, T.T. Zhang, L.S. Qian, X.J. Zhang, G.D. Liu, Gold-platinum nanoflowers as colored and catalytic labels for ultrasensitive lateral flow MicroRNA-21 assay, Sens. Actuator B-Chem. 344 (2021) 7.
[42] P.P. Wang, L. Cao, Y. Chen, Y. Wu, J.W. Di, Photoelectrochemical biosensor based on Co3O4 nanoenzyme coupled with PbS quantum dots for hydrogen peroxide detection, ACS Appl. Nano Mater. 2 (4) (2019) 2204–2211.
[43] Y.J. Zhan, Y.B. Zeng, L. Li, L.H. Guo, F. Luo, B. Qiu, Y.J. Huang, Z.Y. Lin, Cu2+-Modified boron nitride nanosheets-supported subnanometer gold nanoparticles: an oxidase-mimicking nanoenzyme with unexpected oxidation properties, Anal. Chem. 92 (1) (2020) 1236–1244.

[44] D.L. Wei, X.Y. Zhang, B. Chen, K. Zeng, Using bimetallic Au@Pt nanozymes as a visual tag and as an enzyme mimic in enhanced sensitive lateral-flow immunoassays: application for the detection of streptomycin, Anal. Chim. Acta 1126 (2020) 106–113.
[45] H. Abdolmohammad-Zadeh, E. Rahimpour, A novel chemosensor for Ag(I) ion based on its inhibitory effect on the luminol-H2O2 chemiluminescence response improved by CoFe2O4 nano-particles, Sens. Actuator B-Chem. 209 (2015) 496–504.
[46] G. Jiang, H. Liu, J. Liu, L.e. Liu, Y. Li, L. Xue, Y. Wu, R. Yang, Engineering of multifunctional carbon nanodots-decorated plasmonic Au@Ag nanoenzymes for photoelectrochemical biosensing of microRNA-155, Sens. Actuators B-Chem. 360 (2022), 131653.
[47] K.K. Xiang, G. Chen, A.X. Nie, W.J. Wang, H.Y. Han, Silica-based nanoenzymes for rapid and ultrasensitive detection of mercury ions, Sens. Actuator B-Chem. 330 (2021) 7.
[48] A. Jaisankar, S. Krishnan, L. Rangasamy, Recent developments of aptamer-based lateral flow assays for point-of-care (POC) diagnostics, Anal. Biochem. 655 (2022) 22.
[49] N. Zhang, J.R. Li, B.S. Liu, D. Zhang, C.Y. Zhang, Y.H. Guo, X.H. Chu, W.T. Wang, H.X. Wang, X.H. Yan, Z. Li, Signal enhancing strategies in aptasensors for the detection of small molecular contaminants by nanomaterials and nucleic acid amplification, Talanta 236 (2022) 21.
[50] G. Su, M. Zhu, D. Li, M. Xu, Y. Zhu, Y. Zhang, H. Zhu, F. Li, Y. Yu, Multiplexed lateral flow assay integrated with orthogonal CRISPR-Cas system for SARS-CoV-2 detection, Sens. Actuators B-Chem. 371 (2022), 132537.
[51] X. Xia, H. Yang, J. Cao, J. Zhang, Q. He, R. Deng, Isothermal nucleic acid amplification for food safety analysis, TrAC Trends Anal. Chem. (Reference Ed.) 153 (2022), 116641.
[52] L. Sun, P. Li, X.H. Ju, J. Rao, W.Z. Huang, L.L. Ren, S.J. Zhang, T.L. Xiong, K. Xu, X.L. Zhou, M.L. Gong, E. Miska, Q. Ding, J.W. Wang, Q.F.C. Zhang, In vivo structural characterization of the SARS-CoV-2 RNA genome identifies host proteins vulnerable to repurposed drugs, Cell 184 (7) (2021) 1865–1883. E20.
[53] L. Qu, Z.Y. Yi, Y. Shen, L.R. Lin, F. Chen, Y.Y. Xu, Z.G. Wu, H.X. Tang, X.X. Zhang, F. Tian, C.H. Wang, X. Xiao, X.J. Dong, L. Guo, S.Y. Lu, C.Y. Yang, C. Tang, Y. Yang, W.H. Yu, J.B. Wang, Y.A. Zhou, Q. Huang, A. Yisimayi, S. Liu, W. J. Huang, Y.L. Cao, Y.C. Wang, Z. Zhou, X.Z. Peng, J.W. Wang, X.S. Xie, W.S. Wei, Circular RNA vaccines against SARS-CoV-2 and emerging variants, Cell 185 (10) (2022) 1728–1744. E16.
[54] E.H. Ahmed-Abakur, M.F. Ullah, E.H. Elssaig, T.M.S. Alnour, In-silico genomic landscape characterization and evolution of SARS-CoV-2 variants isolated in India shows significant drift with high frequency of mutations, Saudi J. Biol. Sci. 29 (5) (2022) 3494–3501.
[55] J.Y. Zhao, Q. Liu, D.R. Yi, Q.J. Li, S.S. Guo, L. Ma, Y.X. Zhang, D.X. Dong, F. Guo, Z.L. Liu, T. Wei, X.Y. Li, S. Cen, 5-Iodotubercidin inhibits SARS-CoV-2 RNA synthesis, Antivir. Res. 198 (2022) 8.
[56] M. Hasan, A.I. Ashik, M.B. Chowdhury, A.T. Tasnim, Z.S. Nishat, T. Hossain, S. Ahmed, Computational prediction of potential siRNA and human miRNA sequences to silence orf1ab associated genes for future therapeutics against SARS-CoV-2, Inf. Med. unlocked 24 (2021), 100569.
[57] A. Labeau, L. Fery-Simonian, A. Lefevre-Utile, M. Pourcelot, L. Bonnet-Madin, V. Soumelis, V. Lotteau, P.-O. Vidalain, A. Amara, L. Meertens, Characterization and functional interrogation of the SARS-CoV-2 RNA interactome, Cell Rep. 39 (4) (2022), 110744.
[58] J. Herrera-Uribe, P. Naylor, E. Rajab, B. Mathews, G. Coskuner, M.S. Jassim, M. Al-Qahtani, N.J. Stevenson, Long term detection and quantification of SARS-CoV-2 RNA in wastewater in Bahrain, J. Hazard. Mater. Adv. 7 (2022), 100082.
[59] Y. Peng, Y.H. Pan, Z.W. Sun, J.L. Li, Y.X. Yi, J. Yang, G.X. Li, An electrochemical biosensor for sensitive analysis of the SARS-CoV-2 RNA, Biosens. Bioelectron. 186 (2021) 6.
[60] K. Dighe, P. Moitra, M. Alafeef, N. Gunaseelan, D. Pan, A rapid RNA extraction-free lateral flow assay for molecular point-of-care detection of SARS-CoV-2 augmented by chemical probes, Biosens. Bioelectron. 200 (2022) 7.
[61] S. Yu, S.B. Nimse, J. Kim, K.S. Song, T. Kim, Development of a lateral flow strip membrane assay for rapid and sensitive detection of the SARS-CoV-2, Anal. Chem. 92 (20) (2020) 14139–14144.
[62] Y.X. Wang, H. Chen, H.J. Wei, Z. Rong, S.Q. Wang, Tetra-primer ARMS-PCR combined with dual-color fluorescent lateral flow assay for the discrimination of SARS-CoV-2 and its mutations with a handheld wireless reader, Lab Chip 22 (8) (2022) 1531–1541.
[63] X.H. Yang, J. Xie, S.Q. Hu, W.L. Zhan, L. Duan, K.Y. Chen, C.B. Zhang, A.H. Yin, M.Y. Luo, Rapid and visual detection of enterovirus using recombinase polymerase amplification combined with lateral flow strips, Sens. Actuator B-Chem. 311 (2020) 7.
[64] S. Tomar, B. Lavickova, C. Guiducci, Recombinase polymerase amplification in minimally buffered conditions, Biosens. Bioelectron. 198 (2022) 7.
[65] L. Farrera-Soler, A. Gonse, K.T. Kim, S. Barluenga, N. Winssinger, Combining recombinase polymerase amplification and DNA-templated reaction for SARS-CoV-2 sensing with dual fluorescence and lateral flow assay output, Biopolymers 113 (4) (2022) 9.
[66] C.P. Mancuso, Z.X. Lu, J. Qian, S.A. Boswell, M. Springer, A semi-quantitative isothermal diagnostic assay utilizing competitive amplification, Anal. Chem. 93 (27) (2021) 9541–9548.
[67] Y. Sun, P.Z. Qin, J. He, W.W. Li, Y.L. Shi, J.G. Xu, Q. Wu, Q.Q. Chen, W.D. Li, X. X. Wang, G.D. Liu, W. Chen, Rapid and simultaneous visual screening of SARS-CoV-2 and influenza virufses with customized isothermal amplification integrated lateral flow strip, Biosens. Bioelectron. 197 (2022), 113771.
[68] J.S. Kumar, M. Parida, A.M. Shete, T. Majumdar, S. Patil, P.D. Yadav, P.K. Dash, Development of a reverse transcription loop- mediated isothermal amplification RT-LAMP as a early rapid detection assay for crimean Congo hemorrhagic fever virus, Acta Trop. 231 (2022) 6.
[69] M. Varona, D.R. Eitzmann, J.L. Anderson, Sequence-specific detection of ORF1a, BRAF, and ompW DNA sequences with loop mediated isothermal amplification on lateral flow immunoassay strips enabled by molecular beacons, Anal. Chem. 93 (9) (2021) 4149–4153.
[70] A.A.A. Al-maskri, J.W. Ye, J. Talap, H.H. Hu, L.L. Sun, L.S. Yu, S. Cai, S. Zeng, Reverse transcription-based loop-mediated isothermal amplification strategy for real-time miRNA detection with phosphorothioated probes, Anal. Chim. Acta 1126 (2020) 1–6.
[71] A.L. Ge, F.Y. Liu, X.D. Teng, C.J. Cui, F. Wu, W.J. Liu, Y. Liu, X.G. Chen, J. Xu, B. Ma, A Palm Germ-Radar (PaGeR) for rapid and simple COVID-19 detection by reverse transcription loop-mediated isothermal amplification (RT-LAMP), Biosens. Bioelectron. 200 (2022) 9.
[72] M.T. Yang, Y.D. Tang, L.J. Qi, S.C. Zhang, Y.C. Liu, B.Y. Lu, J.X. Yu, K. Zhu, B. L. Li, Y. Du, SARS-CoV-2 point-of-care (POC) diagnosis based on commercial pregnancy test strips and a palm-size microfluidic device, Anal. Chem. 93 (35) (2021) 11956–11964.
[73] X. Zhu, X.X. Wang, L.M. Han, T. Chen, L.C. Wang, H. Li, S. Li, L.F. He, X.Y. Fu, S. J. Chen, M. Xing, H. Chen, Y. Wang, Multiplex reverse transcription loop-mediated isothermal amplification combined with nanoparticle-based lateral flow biosensor for the diagnosis of COVID-19, Biosens, Bioelectron 166 (2020) 7.
[74] S. Banerjee, S.K. Biswas, N. Kedia, R. Sarkar, A. De, S. Mitra, S. Roy, R. Chowdhury, S. Samaddar, A. Bandopadhyay, I. Banerjee, S. Jana, R. Goswami, S. Dutta, M. Chawla-Sarkar, S. Chakraborty, A. Mondal, Piecewise isothermal nucleic acid testing (PINAT) for infectious disease detection with sample-to-result integration at the point-of-care, ACS Sens. 6 (10) (2021) 3753–3764.
[75] L.L. Zhuang, J.S. Gong, M. Ma, Y.X. Ji, P.L. Tian, X.M. Mei, N. Gu, Y. Zhang, Tri-primer-enhanced strand exchange amplification combined with rapid lateral flow fluorescence immunoassay to detect SARS-CoV-2, Analyst 146 (21) (2021) 6650–6664.
[76] H.M. Zhang, K.Y. Wang, S.J. Bu, Z.Y. Li, C.J. Ju, J.Y. Wan, Colorimetric detection of microRNA based on DNAzyme and nuclease-assisted catalytic hairpin assembly signal amplification, Mol. Cell. Probes 38 (2018) 13–18.
[77] A. Mudiyanselage, Q.K. Yu, M.A. Leon-Duque, B. Zhao, R. Wu, M.X. You, Genetically encoded catalytic hairpin assembly for sensitive RNA imaging in live cells, J. Am. Chem. Soc. 140 (28) (2018) 8739–8745.
[78] M.Y. Zou, F.Y. Su, R. Zhang, X.L. Jiang, H. Xiao, X.J. Yan, C.K. Yang, X.B. Fan, G. Q. Wu, Rapid point-of-care testing for SARS-CoV-2 virus nucleic acid detection by an isothermal and nonenzymatic Signal amplification system coupled with a lateral flow immunoassay strip, Sens. Actuator B-Chem. 342 (2021) 8.
[79] Y.C. Pan, X.W. Luan, F. Zeng, Q. Xu, Z.K. Li, Y.F. Gao, X.L. Liu, X.Q. Li, X. Han, J. L. Shen, Y.J. Song, Hollow covalent organic framework-sheltering CRISPR/Cas12a as an in-vivo nanosensor for ATP imaging, Biosens. Bioelectron. 209 (2022) 7.
[80] R. Aman, A. Mahas, M. Mahfouz, Nucleic acid detection using CRISPR/cas biosensing technologies, ACS Synth. Biol. 9 (6) (2020) 1226–1233.
[81] Q. Zhang, J. Li, Y. Li, G. Tan, M. Sun, Y. Shan, Y. Zhang, X. Wang, K. Song, R. Shi, L. Huang, F. Liu, Y. Yi, X. Wu, SARS-CoV-2 detection using quantum dot fluorescence immunochromatography combined with isothermal amplification and CRISPR/Cas13a, Biosens. Bioelectron. 202 (2022), 113978.
[82] X. Zhu, X.X. Wang, S.J. Li, W.K. Luo, X.P. Zhang, C.Z. Wang, Q. Chen, S.Y. Yu, J. Tai, Y. Wang, Rapid, ultrasensitive, and highly specific diagnosis of COVID-19 by CRISPR-based detection, ACS Sens. 6 (3) (2021) 881–888.
[83] G.H. Cao, D.Q. Huo, X.L. Chen, X.F. Wang, S.Y. Zhou, S.X. Zhao, X.G. Luo, C. J. Hou, Automated, portable, and high-throughput fluorescence analyzer (APHF-analyzer) and lateral flow strip based on CRISPR/Cas13a for sensitive and visual detection of SARS-CoV-2, Talanta 248 (2022) 9.
[84] E. Xiong, L. Jiang, T.A. Tian, M.L. Hu, H.H. Yue, M.Q. Huang, W. Lin, Y.Z. Jiang, D.B. Zhu, X.M. Zhou, Simultaneous dual-gene diagnosis of SARS-CoV-2 based on CRISPR/Cas9-Mediated lateral flow assay, Angew. Chem.-Int. Edit. 60 (10) (2021) 5307–5315.
[85] Z. Ali, E. Sanchez, M. Tehseen, A. Mahas, T. Marsic, R. Aman, G.S. Rao, F. S. Alhamlan, M.S. Alsanea, A.A. Al-Qahtani, S. Hamdan, M. Mahfouz, Bio-SCAN: a CRISPR/dCas9-based lateral flow assay for rapid, specific, and sensitive detection of SARS-CoV-2, ACS Synth. Biol. 11 (1) (2022) 406–419.
[86] C.S. He, C.L. Lin, G.S. Mo, B.B. Xi, A.A. Li, D.C. Huang, Y.B. Wan, F. Chen, Y. F. Liang, Q.X. Zuo, W.Q. Xu, D.Y. Feng, G.T. Zhang, L.Y. Han, C.W. Ke, H.L. Du, L. Z. Huang, Rapid and accurate detection of SARS-CoV-2 mutations using a Cas12a-based sensing platform, Biosens. Bioelectron. 198 (2022), 113857.
[87] S.J. Li, J.F. Huang, L.J. Ren, W.J. Jiang, M. Wang, L. Zhuang, Q.N. Zheng, R. Yang, Y. Zeng, L.D.W. Luu, Y. Wang, J. Tai, A one-step, one-pot CRISPR nucleic acid detection platform (CRISPR-top): application for the diagnosis of COVID-19, Talanta 233 (2021), 122591.
[88] G. Li, W.P. Li, X.L. Fang, X.R. Song, S.J. Teng, Z. Ren, D.Q. Hu, S.H. Zhou, G. Q. Wu, K.Q. Li, Expression and purification of recombinant SARS-CoV-2 nucleocapsid protein in inclusion bodies and its application in serological detection, Protein Expr. Purif. 186 (2021), 105908.
[89] Y. Xu, C. Xia, X. Zeng, Y.L. Qiu, M.J. Liao, Q. Jiang, M.F. Quan, R.S. Liu, Development of magnetic particle-based chemiluminescence immunoassay for measurement of SARS-CoV-2 nucleocapsid protein, J. Virol. Methods 302 (2022), 114486.

[90] G. Tatar, E. Ozyurt, K. Turhan, Computational drug repurposing study of the RNA binding domain of SARS-CoV-2 nucleocapsid protein with antiviral agents, Biotechnol. Prog. 37 (2) (2021), e3110.
[91] N. Kumar, N.P. Shetti, S. Jagannath, T.M. Aminabhavi, Electrochemical sensors for the detection of SARS-CoV-2 virus, Chem. Eng. J. 430 (2022), 132966.
[92] M. Dang, Y.F. Li, J.X. Song, ATP biphasically modulates LLPS of SARS-CoV-2 nucleocapsid protein and specifically binds its RNA-binding domain, Biochem. Biophys. Res. Commun. 541 (2021) 50–55.
[93] I.P. Caruso, V.D. Almeida, M.J. do Amaral, G.C. de Andrade, G.R. de Araujo, T. S. de Araujo, J.M. de Azevedo, G.M. Barbosa, L. Bartkevihi, P.R. Bezerra, K.M. D. Cabral, I.O. de Lourenco, C.L.F. Malizia-Motta, A.D. Marques, N.C. Mebus-Antunes, T.C. Neves-Martins, J.M. de Sa, K. Sanches, M.C. Santana-Silva, A. A. Vasconcelos, M.D. Almeida, G.C. de Amorim, C.D. Anobom, A.T. Da Poian, F. Gomes-Neto, A.S. Pinheiro, F.C.L. Almeida, Insights into the specificity for the interaction of the promiscuous SARS-CoV-2 nucleocapsid protein N-terminal domain with deoxyribonucleic acids, Int. J. Biological Macromol. 203 (2022) 466–480.
[94] M. Biswal, J.W. Lu, J.K. Song, SARS-CoV-2 nucleocapsid protein targets a conserved surface groove of the NTF2-like domain of G3BP1, J. Mol. Biol. 434 (9) (2022).
[95] L.J. Sherwood, A. Hayhurst, Toolkit for quickly generating and characterizing molecular probes specific for SARS-CoV-2 nucleocapsid as a primer for future coronavirus pandemic preparedness, ACS Synth. Biol. 10 (2) (2021) 379–390.
[96] W.H. Khan, N. Khan, A. Mishra, S. Gupta, V. Bansode, D. Mehta, R. Bhambure, M. A. Ansari, S. Das, A.S. Rathore, Dimerization of SARS-CoV-2 nucleocapsid protein affects sensitivity of ELISA based diagnostics of COVID-19, Int. J. Biological Macromol. 200 (2022) 428–437.
[97] M.S. Rahman, M.R. Islam, A. Ul Alam, I. Islam, M.N. Hoque, S. Akter, M. M. Rahaman, M. Sultana, M.A. Hossain, Evolutionary dynamics of SARS-CoV-2 nucleocapsid protein and its consequences, J. Med. Virol. 93 (4) (2021) 2177–2195.
[98] Y. Yamaoka, K. Miyakawa, S.S. Jeremiah, R. Funabashi, K. Okudela, S. Kikuchi, J. Katada, A. Wada, T. Takei, M. Nishi, K. Shimizu, H. Ozawa, S. Usuku, C. Kawakami, N. Tanaka, T. Morita, H. Hayashi, H. Mitsui, K. Suzuki, D. Aizawa, Y. Yoshimura, T. Miyazaki, E. Yamazaki, T. Suzuki, H. Kimura, H. Shimizu, N. Okabe, H. Hasegawa, A. Ryo, Highly specific monoclonal antibodies and epitope identification against SARS-CoV-2 nucleocapsid protein for antigen detection tests, Cell Rep. Med. 2 (6) (2021), 100311.
[99] A.H. Lyu, T.C. Jin, S.S. Wang, X.X. Huang, W.H. Zeng, R. Yang, H. Cui, Automatic label-free immunoassay with high sensitivity for rapid detection of SARS-CoV-2 nucleocapsid protein based on chemiluminescent magnetic beads, Sens. Actuator B-Chem. 349 (2021), 130739.
[100] H.K. Oh, K. Kim, J. Park, H. Im, S. Maher, M.G. Kim, Plasmon color-preserved gold nanoparticle clusters for high sensitivity detection of SARS-CoV-2 based on lateral flow immunoassay, Biosens. Bioelectron. 205 (2022), 114094.
[101] L. Shen, Q.H. Zhang, X.L. Luo, H.L. Xiao, M. Gu, L.L. Cao, F.J. Zhao, Z.C. Chen, A rapid lateral flow immunoassay strip for detection of SARS-CoV-2 antigen using latex microspheres, J. Clin. Lab. Anal. 35 (12) (2021), e24091.
[102] L.D. Xu, J. Zhu, S.N.A. Ding, Immunoassay of SARS-CoV-2 nucleocapsid proteins using novel red emission-enhanced carbon dot-based silica spheres, Analyst 146 (16) (2021) 5055–5060.
[103] C.W. Wang, X.D. Cheng, L.Y. Liu, X.C. Zhang, X.S. Yang, S. Zheng, Z. Rong, S. Q. Wang, Ultrasensitive and simultaneous detection of two specific SARS-CoV-2 antigens in human specimens using direct/enrichment dual-mode fluorescence lateral flow immunoassay, ACS Appl. Mater. Interfaces 13 (34) (2021) 40342–40353.
[104] Z. Xie, S. Feng, F. Pei, M. Xia, Q. Hao, B. Liu, Z. Tong, J. Wang, W. Lei, X. Mu, Magnetic/fluorescent dual-modal lateral flow immunoassay based on multifunctional nanobeads for rapid and accurate SARS-CoV-2 nucleocapsid protein detection, Anal. Chim. Acta 1233 (2022), 340486.
[105] Y.B. Yan, J.C. Zhang, S.H. Yi, L. Liu, C.X. Huang, Lighting up forensic science by aggregation-induced emission: a review, Anal. Chim. Acta 1155 (2021), 238119.
[106] G.Q. Zhang, Z.Y. Gao, J.T. Zhang, H.L. Ou, H.Q. Gao, R.T.K. Kwok, D. Ding, B. Z. Tang, A wearable AIEgen-based lateral flow test strip for rapid detection of SARS-CoV-2 RBD protein and N protein, Cell Rep. Phys. Sci. 3 (2) (2022), 100740.
[107] B.D. Grant, C.E. Anderson, J.R. Williford, L.F. Alonzo, V.A. Glukhova, D.S. Boyle, B.H. Weigl, K.P. Nichols, SARS-CoV-2 coronavirus nucleocapsid antigen-detecting half-strip lateral flow assay toward the development of point of care tests using commercially available reagents, Anal. Chem. 92 (16) (2020) 11305–11309.
[108] D.W. Bradbury, J.T. Trinh, M.J. Ryan, C.M. Cantu, J.K. Lu, F.D. Nicklen, Y.S. Du, R. Sun, B.M. Wu, D.T. Kamei, On-demand nanozyme signal enhancement at the push of a button for the improved detection of SARS-CoV-2 nucleocapsid protein in serum, Analyst 146 (24) (2021) 7386–7393.
[109] Y.Y. Hui, Y.X. Tang, T. Azuma, H.H. Lin, F.Z. Liao, Q.Y. Chen, J.H. Kuo, Y. L. Wang, H.C. Chang, Design and implementation of a low-cost portable reader for thermometric lateral flow immunoassay, J. Chin. Chem. Soc. 69 (8) (2022) 1356–1365.
[110] H. Han, C. Wang, X. Yang, S. Zheng, X. Cheng, Z. Liu, B. Zhao, R. Xiao, Rapid field determination of SARS-CoV-2 by a colorimetric and fluorescent dual-functional lateral flow immunoassay biosensor, Sens. Actuators-B, Chem. 351 (2022), 130897.
[111] A.N. Baker, S.J. Richards, C.S. Guy, T.R. Congdon, M. Hasan, A.J. Zwetsloot, A. Gallo, J.R. Lewandowski, P.J. Stansfeld, A. Straube, M. Walker, S. Chessa, G. Pergolizzi, S. Dedola, R.A. Field, M.I. Gibson, The SARS-COV-2 spike protein binds sialic acids and enables rapid detection in a lateral flow point of care diagnostic device, ACS Cent. Sci. 6 (11) (2020) 2046–2052.
[112] S.H. Kim, F.L. Kearns, M.A. Rosenfeld, L. Casalino, M.J. Papanikolas, C. Simmerling, R.E. Amaro, R. Freeman, GlycoGrip: cell surface-inspired universal sensor for betacoronaviruses, ACS Cent. Sci. 8 (1) (2022) 22–42.
[113] L.F. Yang, N. Kacherovsky, N. Panpradist, R. Wan, J. Liang, B. Zhang, S. J. Salipante, B.R. Lutz, S.H. Pun, Aptamer sandwich lateral flow assay (AptaFlow) for antibody-free SARS-CoV-2 detection, Anal. Chem. 94 (20) (2022) 7278–7285.
[114] J.H. Lee, M. Choi, Y. Jung, S.K. Lee, C.S. Lee, J. Kim, J. Kim, N.H. Kim, B.T. Kim, H.G. Kim, A novel rapid detection for SARS-CoV-2 spike 1 antigens using human angiotensin converting enzyme 2 (ACE2), Biosens. Bioelectron. 171 (2021), 112715.
[115] G.B. Chand, A. Banerjee, G.K. Azad, Identification of twenty-five mutations in surface glycoprotein (Spike) of SARS-CoV-2 among Indian isolates and their impact on protein dynamics, Gene reports 21 (2020), 100891.
[116] L.M. Miller, L.F. Barnes, S.A. Raab, B.E. Draper, T.J. El-Baba, C.A. Lutomski, C. V. Robinson, D.E. Clemmer, M.F. Jarrold, Heterogeneity of glycan processing on trimeric SARS-CoV-2 spike protein revealed by charge detection mass spectrometry, J. Am. Chem. Soc. 143 (10) (2021) 3959–3966.
[117] Y.W. Cheng, T.L. Chao, C.L. Li, M.F. Chiu, H.C. Kao, S.H. Wang, Y.H. Pang, C. H. Lin, Y.M. Tsai, W.H. Lee, M.H. Tao, T.C. Ho, P.Y. Wu, L.T. Jang, P.J. Chen, S. Y. Chang, S.H. Yeh, Furin inhibitors block SARS-CoV-2 spike protein cleavage to suppress virus production and cytopathic effects, Cell Rep. 33 (2) (2020), 108254.
[118] K. Guruprasad, Mutations in human SARS-CoV-2 spike proteins, potential drug binding and epitope sites for COVID-19 therapeutics development, Current Res. Struct. Biol. 4 (2022) 41–50.
[119] A. Sternberg, C. Naujokat, Structural features of coronavirus SARS-CoV-2 spike protein: targets for vaccination, Life Sci. 257 (2020), 118056.
[120] N. Suryadevara, S. Shrihari, P. Gilchuk, L.A. VanBlargan, E. Binshtein, S.J. Zost, R.S. Nargi, R.E. Sutton, E.S. Winkler, E.C. Chen, M.E. Fouch, E. Davidson, B. J. Doranz, R.E. Chen, P.Y. Shi, R.H. Carnahan, L.B. Thackray, M.S. Diamond, J. E. Crowe, Neutralizing and protective human monoclonal antibodies recognizing the N-terminal domain of the SARS-CoV-2 spike protein, Cell 184 (9) (2021) 2316–2331, e15.
[121] J.G.d.O. Santos, D.P. Migueis, J.B.d. Amaral, A.L.L. Bachi, A.C. Boggi, A. Thamboo, R.L. Voegels, R. Pezato, Impact of SARS-CoV-2 on saliva: TNF-α, IL-6, IL-10, lactoferrin, lysozyme, IgG, IgA, and IgM, J. Oral Biosci. 64 (1) (2022) 108–113.
[122] C. Chu, A. Schonbrunn, S. Elitok, F. Kern, K. Schnatbaum, H. Wenschuh, K. Klemm, V. von Baehr, B.K. Kramer, B. Hocher, T-cell proliferation assay for the detection of SARS-CoV-2-specific T-cells, Clin. Chim. Acta 532 (2022) 130–136.
[123] M. Kurano, Y. Morita, Y. Nakano, R. Yokoyama, T. Shimura, C.G. Qian, F.Z. Xia, F. He, L. Zheng, H. Ohmiya, Y. Kishi, J. Okada, N. Yoshikawa, K. Nakajima, Y. Nagura, H. Okazaki, D. Jubishi, K. Moriya, Y. Seto, F. Yasui, M. Kohara, M. Wakui, T. Kawamura, T. Kodama, Y. Yatomi, Response kinetics of different classes of antibodies to SARS-CoV2 infection in the Japanese population: the IgA and IgG titers increased earlier than the IgM titers, Int. Immunopharm. 103 (2022), 108491.
[124] B. Crescenzo-Chaigne, S. Behillil, V. Enouf, N. Escriou, S. Petres, M.N. Ungeheuer, J. Ghosn, S. Tubiana, L. Bouadma, S. van der Werf, C. Demeret, C.c.s.g. French, Nasopharyngeal and serological anti SARS-CoV-2 IgG/IgA responses in COVID-19 patients, J. Clinical Virol. plus 1 (4) (2021), 100041.
[125] G. Brisotto, E. Muraro, M. Montico, C. Corso, C. Evangelista, M. Casarotto, C. Caffau, R. Vettori, M.R. Cozzi, S. Zanussi, M. Turetta, F. Ronchese, A. Steffan, IgG antibodies against SARS-CoV-2 decay but persist 4 months after vaccination in a cohort of healthcare workers, Clin. Chim. Acta 523 (2021) 476–482.
[126] A. Ruggiero, C. Piubelli, L. Calciano, S. Accordini, M.T. Valenti, L.D. Carbonare, G. Siracusano, N. Temperton, N. Tiberti, S.S. Longoni, M. Pizzato, S. Accordini, T. Fantoni, L. Lopalco, A. Beretta, Z. Bisof, D. Zipeto, D. Group, SARS-CoV-2 vaccination elicits unconventional IgM specific responses in naive and previously COVID-19-infected individuals, EBioMedicine 77 (2022), 103888.
[127] X.Q. Yan, S.J. Zhu, Z.X. Jin, G.Q. Chen, Z.W. Zhang, J.M. He, S.Q. Yin, K. Peng, W. W. Xiao, Z.L. Zhou, R.F. Gui, F. Chen, Y. Cao, Y.C. Zhou, Z.Y. Li, Y. Zeng, X. T. Han, Y.M. Zhu, Persistence of anti-SARS-CoV-2 IgM in convalescent COVID-19 patients, J. Infect. 84 (1) (2022) E29–E32.
[128] A.C. Nilsson, D.K. Holm, U.S. Justesen, T. Gorm-Jensen, N.S. Andersen, A. Ovrehus, I.S. Johansen, J. Michelsen, U. Sprogoe, S.T. Lillevang, Comparison of six commercially available SARS-CoV-2 antibody assays-Choice of assay depends on intended use, Int. J. Infect. Dis. 103 (2021) 381–388.
[129] M.A. Sughayer, L. Souan, M.M. Abu Alhowr, D. Al Rimawi, M. Siag, S. Albadr, M. Owdeh, T. Al Atrash, Comparison of the effectiveness and duration of anti-RBD SARS-CoV-2 IgG antibody response between different types of vaccines: implications for vaccine strategies, Vaccine 40 (20) (2022) 2841–2847.
[130] H. Guo, Q. Fan, S. Song, S. Shen, B. Zhou, H. Wang, L. Cheng, X. Ge, B. Ju, Z. Zhang, Increased resistance of SARS-CoV-2 Lambda variant to antibody neutralization, J. Clin. Virol.: the official publication of the Pan American Society for Clinical Virology 150–151 (2022), 105162.
[131] T. Wen, C. Huang, F.J. Shi, X.Y. Zeng, T. Lu, S.N. Ding, Y.J. Jiao, Development of a lateral flow immunoassay strip for rapid detection of IgG antibody against SARS-CoV-2 virus, Analyst 145 (15) (2020) 5345–5352.
[132] C. Huang, T. Wen, F.J. Shi, X.Y. Zeng, Y.J. Jiao, Rapid detection of IgM antibodies against the SARS-CoV-2 virus via colloidal gold nanoparticle-based lateral-flow assay, ACS Omega 5 (21) (2020) 12550–12556.
[133] Y.F. Zhou, Y. Chen, Y. Liu, H. Fang, X.L. Huang, Y.K. Leng, Z.Q. Liu, L. Hou, W. Zhang, W.H. Lai, Y.H. Xiong, Controlled copper in situ growth-amplified lateral flow sensors for sensitive, reliable, and field-deployable infectious disease diagnostics, Biosens. Bioelectron. 171 (2021), 112753.

[134] B. Gosselin, M. Retout, R. Dutour, L. Troian-Gautier, R. Bevernaegie, S. Herens, P. Lefevre, O. Denis, G. Bruylants, I. Jabin, Ultrastable silver nanoparticles for rapid serology detection of anti-SARS-CoV-2 immunoglobulins G, Anal. Chem. 94 (20) (2022) 7383–7390.
[135] E. Diani, P.P. Piccaluga, V. Lotti, A. Di Clemente, M. Ligozzi, P. De Nardo, L. Lambertenghi, F. Pizzolo, S. Friso, G. Lo Cascio, A. Vianello, G. Marchi, E. Concia, D. Gibellini, Assessment of SARS-CoV-2 IgG and IgM antibody detection with a lateral flow immunoassay test, Heliyon 7 (10) (2021), e08192.
[136] M.A. Black, G.M. Shen, X.J. Feng, W.F.G. Beltran, Y. Feng, V. Vasudevaraja, D. Allison, L.H. Lin, T. Gindin, M. Astudillo, D.N. Yang, M. Murali, A.J. Iafrate, G. Jour, P. Cotzia, M. Snuderl, Analytical performance of lateral flow immunoassay for SARS-CoV-2 exposure screening on venous and capillary blood samples, J. Immunol. Methods 489 (2021), 112909.
[137] Z.T. Li, Y.X. Yi, X.M. Luo, N. Xiong, Y. Liu, S.Q. Li, R.L. Sun, Y.Q. Wang, B.C. Hu, W. Chen, Y.C. Zhang, J. Wang, B.F. Huang, Y. Lin, J.S. Yang, W.S. Cai, X.F. Wang, J. Cheng, Z.Q. Chen, K.J. Sun, W.M. Pan, Z.F. Zhan, L.Y. Chen, F. Ye, Development and clinical application of a rapid IgM-IgG combined antibody test for SARS-CoV-2 infection diagnosis, J. Med. Virol. 92 (9) (2020) 1518–1524.
[138] L. Zeng, Y. Li, J. Liu, L.L. Guo, Z.X. Wang, X.X. Xu, S.S. Song, C.L. Hao, L.Q. Liu, M.G. Xin, C.L. Xu, Rapid, ultrasensitive and highly specific biosensor for the diagnosis of SARS-CoV-2 in clinical blood samples, Mater. Chem. Front. 4 (7) (2020) 2000–2005.
[139] J. Liu, W. Yan, Z. Liu, Y. Han, Y. Xia, J. Yu, A colloidal gold-based immunochromatographic strip for rapid detection of SARS-CoV-2 antibodies after vaccination, Med. Novel Technol. Devices 11 (2021), 100084.
[140] R.Y. Alhabbab, M.A. Alfaleh, R.M. Alsulaiman, S.S. Alamri, M.S. Eyouni, M. Z. ElAssouli, A.M. Abuzenadah, A.M. Hashem, Amplifying lateral flow assay signals for rapid detection of COVID-19 specific antibodies, Glob. Chall. 6 (7) (2022), 2200008.
[141] Z.Z. Wang, Z. Zheng, H.Z. Hu, Q.W. Zhou, W. Liu, X.Q. Li, Z.G. Liu, Y.H. Wang, Y. F. Ma, A point-of-care selenium nanoparticle-based test for the combined detection of anti-SARS-CoV-2 IgM and IgG in human serum and blood, Lab Chip 20 (22) (2020) 4255–4261.
[142] Z.H. Chen, Z.G. Zhang, X.M. Zhai, Y.Y. Li, L. Lin, H. Zhao, L. Bian, P. Li, L. Yu, Y. S. Wu, G.F. Lin, Rapid and sensitive detection of anti-SARS-CoV-2 IgG, using lanthanide-doped nanoparticles-based lateral flow immunoassay, Anal. Chem. 92 (10) (2020) 7226–7231.
[143] X.J. Duan, Y.J. Shi, X.D. Zhang, X.X. Ge, R. Fan, J.H. Guo, Y.B. Li, G.G. Li, Y. W. Ding, R.A. Osman, W.C. Jiang, J.L. Sun, X. Luan, G.J. Zhang, Dual-detection fluorescent immunochromatographic assay for quantitative detection of SARS-CoV-2 spike RBD-ACE2 blocking neutralizing antibody, Biosens. Bioelectron. 199 (2022), 113883.
[144] C.W. Wang, D.W. Shi, N. Wan, X.S. Yang, H.F. Liu, H.X. Gao, M.L. Zhang, Z.K. Bai, D.C. Li, E.H. Dai, Z. Rong, S.Q. Wang, Development of spike protein-based fluorescence lateral flow assay for the simultaneous detection of SARS-CoV-2 specific IgM and IgG, Analyst 146 (12) (2021) 3908–3917.
[145] J.H. Jia, L.J. Ao, Y.X. Luo, T. Liao, L. Huang, D. Zhuo, C.X. Jiang, J. Wang, J. Hu, Quantum dots assembly enhanced and dual-antigen sandwich structured lateral flow immunoassay of SARS-CoV-2 antibody with simultaneously high sensitivity and specificity, Biosens. Bioelectron. 198 (2022) 8.
[146] R. Chen, C.P. Ren, M. Liu, X.P. Ge, M.S. Qu, X.B. Zhou, M.F. Liang, Y. Liu, F.Y. Li, Early detection of SARS-CoV-2 seroconversion in humans with aggregation-induced near-infrared emission nanoparticle-labeled lateral flow immunoassay, ACS Nano 15 (5) (2021) 8996–9004.
[147] G. Wang, L.M. Yang, C.B. Li, H. Yu, Z.T. He, C.Y. Yang, J.M. Sun, P.F. Zhang, X. G. Gu, B.Z. Tang, Novel strategy to prepare fluorescent polymeric nanoparticles based on aggregation-induced emission via precipitation polymerization for fluorescent lateral flow assay, Mater. Chem. Front. 5 (5) (2021) 2452–2458.
[148] J. Li, B. Liu, X. Tang, Z. Wu, J. Lu, C. Liang, S. Hou, L. Zhang, T. Li, W. Zhao, Y. Fu, Y. Ke, C. Li, Development of a smartphone-based quantum dot lateral flow immunoassay strip for ultrasensitive detection of anti-SARS-CoV-2 IgG and neutralizing antibodies, Int. J. Infect. Dis. 121 (2022) 58–65.
[149] Y.F. Zhou, Y. Chen, W.J. Liu, H. Fang, X.M. Li, L. Hou, Y.J. Liu, W.H. Lai, X. L. Huang, Y.H. Xiong, Development of a rapid and sensitive quantum dot nanobead-based double-antigen sandwich lateral flow immunoassay and its clinical performance for the detection of SARS-CoV-2 total antibodies, Sens. Actuator B-Chem. 343 (2021), 130139.
[150] L.Y. Ye, X.X. Xu, S.S. Song, L.G. Xu, H. Kuang, C.A.L. Xu, Rapid colloidal gold immunochromatographic assay for the detection of SARS-CoV-2 total antibodies after vaccination, J. Mater. Chem. B 10 (11) (2022) 1786–1794.
[151] A. Roda, S. Cavalera, F. Di Nardo, D. Calabria, S. Rosati, P. Simoni, B. Colitti, C. Baggiani, M. Roda, L. Anfossi, Dual lateral flow optical/chemiluminescence immunosensors for the rapid detection of salivary and serum IgA in patients with COVID-19 disease, Biosens. Bioelectron. 172 (2021), 112765.
[152] H.F. Liu, E.H. Dai, R. Xiao, Z.H. Zhou, M.L. Zhang, Z.K. Bai, Y. Shao, K.Z. Qi, J. Tu, C.W. Wang, S.Q. Wang, Development of a SERS-based lateral flow immunoassay for rapid and ultra-sensitive detection of anti-SARS-CoV-2 IgM/IgG in clinical samples, Sens. Actuator B-Chem. 329 (2021), 129196.
[153] S.L. Chen, L.W. Meng, L.T. Wang, X.X. Huang, S. Ali, X.J. Chen, M.G. Yu, M. Yi, L. M. Li, X. Chen, L.M. Yuan, W. Shi, G.Z. Huang, SERS-based lateral flow immunoassay for sensitive and simultaneous detection of anti-SARS-CoV-2 IgM and IgG antibodies by using gap-enhanced Raman nanotags, Sens. Actuator B-Chem. 348 (2021), 130706.
[154] S. Srivastav, A. Dankov, M. Adanalic, R. Grzeschik, V. Tran, S. Pagel-Wieder, F. Gessler, I. Spreitzer, T. Scholz, B. Schnierle, O.E. Anastasiou, U. Dittmer, S. Schlucker, Rapid and sensitive SERS-based lateral flow test for SARS-CoV2-specific IgM/IgG antibodies, Anal. Chem. 93 (36) (2021) 12391–12399.
[155] Q.G. Bayin, L. Huang, C.H. Ren, Y.S. Fu, X. Ma, J.H. Guo, Anti-SARS-CoV-2 IgG and IgM detection with a GMR based LFIA system, Talanta 227 (2021), 122207.
[156] Y.H. Wu, Y.F. Zhou, Y.K. Leng, W.H. Lai, X.L. Huang, Y.H. Xiong, Emerging design strategies for constructing multiplex lateral flow test strip sensors, Biosens. Bioelectron. 157 (2020) 13.
[157] V.T. Nguyen, S. Song, S. Park, C. Joo, Recent advances in high-sensitivity detection methods for paper-based lateral-flow assay, Biosens. Bioelectron. 152 (2020) 17.
[158] W. Deenin, A. Yakoh, C. Kreangkaiwal, O. Chailapakul, K. Patarakul, S. Chaiyo, Integrated lateral flow electrochemical strip for leptospirosis diagnosis, Anal. Chem. 94 (5) (2022) 2554–2560.
[159] J. Sivakumar, J.H. Yang, M.S. Kelly, A. Koh, D. Won, An automated lateral flow assay identification framework: exploring the challenges of a wearable lateral flow assay in mobile application, Expert Syst. Appl. 210 (2022), 118471.
[160] N. Jiang, N.D. Tansukawat, L. Gonzalez-Macia, H.C. Ates, C. Dincer, F. Guder, S. Tasoglu, A.K. Yetisen, Low-cost optical assays for point-of-care diagnosis in resource-limited settings, ACS Sens. 6 (6) (2021) 2108–2124.